PRODUCTION OF TITANIUM DIBORIDE

A THESIS SUBMITTED TO
THE GRADUATE SCHOOL OF NATURAL AND APPLIED SCIENCES
OF
MIDDLE EAST TECHNICAL UNIVERSITY

BY

EDA BİLGİ

IN PARTIAL FULFILLMENT OF THE REQUIREMENTS
FOR
THE DEGREE OF MASTER OF SCIENCE
IN
METALLURGICAL AND MATERIALS ENGINEERING

JANUARY 2007

Approval of the Graduate School of Natural and Applied Sciences

Prof. Dr. Canan Özgen
Director

I certify that this thesis satisfies all the requirements as a thesis for the degree of Master of Science.

Prof. Dr. Tayfur Öztürk
Head of Department

This is to certify that we have read this thesis and that in our opinion it is fully adequate, in scope and quality, as a thesis and for the degree of Master of Science in Metallurgical and Materials Engineering

Prof. Dr. Naci Sevinç
Supervisor

Examining Committee Members

Prof. Dr. Ahmet Geveci (METU, METE) _____

Prof. Dr. Naci Sevinç (METU, METE) _____

Prof. Dr. Yavuz A. Topkaya (METU, METE) _____

Prof.Dr. İshak Karakaya (METU, METE) _____

Prof. Dr. Ali İhsan Arol (METU, MINE) _____

I hereby declare that all information in this document has been obtained and presented in accordance with academic rules and ethical conduct. I also declare that, as required by these rules and conduct, I have fully cited and referenced all material and results that are not original to this work.

Name, Last name : Eda Bilgi

Signature   :

ABSTRACT

PRODUCTION OF TITANIUM DIBORIDE

Bilgi, Eda

M.S., Department of Metallurgical and Materials Engineering

Supervisor : Prof. Dr. Naci Sevinç

January 2007, 78 pages

Titanium diboride was produced both by volume combustion synthesis (VCS) and by mechanochemical synthesis through the reaction of TiO_2, B_2O_3 and metallic Mg. Reaction products were expected to be composed of TiB_2 and MgO. However, side products such as Mg_2TiO_4, $Mg_3B_2O_6$, MgB_2 and TiN were also present in the products obtained by volume combustion synthesis. Formation of TiN could be prevented by conducting the volume combustion synthesis under argon atmosphere. Mg_2TiO_4 did not form when 40% excess Mg was used. Wet ball milling of the products before leaching was found to be effective in removal of $Mg_3B_2O_6$ during leaching in 1M HCl. When stoichiometric starting mixtures were used, all of the side products could be removed after wet ball milling in ethanol and leaching in 5 M HCl. Thus, pure TiB_2 was obtained with a molar yield of 30%. Pure TiB_2 could also be obtained at a molar yield of 45.6% by hot leaching of VCS products at $75^{o}C$ in 5 M HCl, omitting the wet ball milling step. By mechanochemical processing, products containing only TiB_2 and MgO were obtained after 15 hours of ball milling. Leaching in 0.5 M HCl for 3 minutes was found to be sufficient for elimination of MgO. Molar yield of TiB_2 was 89.6%, much higher than that of TiB_2 produced by

volume combustion synthesis. According to scanning electron microscope analyses, produced TiB_2 had average particle size of $0.27\pm0.08\ \mu m$.

Keywords: titanium diboride, volume combustion synthesis, mechanochemical processing, acid leaching.

ÖZ

TİTANYUM DİBORÜR ÜRETİMİ

Bilgi, Eda

Yüksek Lisans, Metalurji ve Malzeme Mühendisliği Bölümü

Tez Yöneticisi: Prof. Dr. Naci Sevinç

Ocak 2007, 78 sayfa

Titanyum diborür hacimsel tutuşma sentezlemesi ve mekanokimyasal işlem yardımıyla TiO_2, B_2O_3 ve Mg arasındaki reaksiyon kullanılarak üretilmiştir. Reaksiyon ürünleri olarak TiB_2 ve MgO fazlarının yanı sıra Mg_2TiO_4, $Mg_3B_2O_6$, MgB_2 ve TiN gibi yan fazlar da gözlenmiştir. TiN oluşumu hacimsel tutuşma deneylerinin argon atmosferinde yapılması ile engellenmiştir. Mg_2TiO_4 fazı % 40 fazla magnezyum eklendiğinde oluşmamıştır. Liç öncesi ıslak öğütme yapılması, $Mg_3B_2O_6$ fazının 1 M HCl içinde liç edilip temizlenmesinde etkili bulunmuştur. Stokiometrik başlangıç malzemeleri kullanıldığı zaman tüm yan fazlar ıslak öğütme ve 5 M HCl içinde liç edildiğinde gitmiştir. Böylece saf titanyum diborür % 30 molar verim ile üretilmiştir. Ayrıca saf titanyum diborür ıslak öğütme işlemi yapılmadan hacimsel tutuşma sentezlemesi yapılmış ürünün 75°C de sıcak 5 M HCl içinde liçi ile de üretilebilmiştir. Bu işlem için molar verim %45,6' dır. Mekanokimyasal işlem ile 15 saat öğütme sonrası sadece TiB_2 ve MgO içeren ürün elde edilmiştir. 0,5 M HCl içinde 3 dakika liç işlemi MgO' ın giderilmesi için yeterli bulunmuştur. Bu yöntemle üretilmiş titanyum diborürün molar verimi % 89,6 olmuştur. Bu değer hacimsel

tutuşma sentezlemesi ile üretilmiş TiB_2' nin molar veriminden daha yüksektir. Tarama elektron mikroskobu analizlerine göre üretilen TiB_2 ortalama 0,27±0,08 µm parçacık büyüklüğüne sahiptir.

Anahtar Kelimeler: titanyum diborür, hacimsel tutuşma sentezlemesi, mekanokimyasal işlem, asit liçi.

To My Parents, My Brother

and My Twin Sister

ACKNOWLEDGMENTS

TABLE OF CONTENTS

LIST OF TABLES

LIST OF FIGURES

CHAPTER I

INTRODUCTION

Solid materials can be classified as metals, ceramics and polymers according to their chemical make-ups and atomic structures [1]. Among them, ceramic compounds are composed of metallic and nonmetallic elements. The most commonly known ceramics are oxides (Al_2O_3, MgO, TiO_2, ZrO_2, SiO_2, etc.), carbides (TiC, WC, B_4C, SiC, etc.), nitrides (Si_3N_4, AlN, BN, TiN, etc.), and borides (TiB_2, ZrB_2, LaB_6, etc.) [1].

Borides, one of the most important types of refractory binary compounds, have been investigated by many researchers during and after the Second World War. These investigations have revealed that these materials have very promising chemical, thermal and electrical properties which make them attractive for various applications [2].

Titanium diboride (TiB_2) is a transition-metal boride which has important chemical, electrical, thermal and mechanical properties. It is the most stable among the several titanium-boron compounds [3]. It has high hardness, high electrical conductivity, thermal stability, and high wear resistance [4, 5]. Moreover, TiB_2 exhibits high elastic modulus and high melting point [6]. Furthermore, it is chemically inert to molten metals [7]. Because this ceramic material has many attractive properties, it is utilized in a variety of applications including cutting tools, wear parts [8], and armor

material [9]. In addition to these application areas, it is used as a cathode material in electrolytic production of aluminum due to its chemical stability [10-12].

There are a number of methods to produce TiB_2. It may be formed as a result of solid state reaction between titanium and boron [11]. In addition, it is possible to produce TiB_2 from reduction of oxides using carbon, boron carbide, magnesium or aluminum as a reducing agent. Electrolysis, vapor phase deposition and mechanochemical synthesis are other techniques for preparation of titanium diboride.

In this study, it was aimed to produce TiB_2, by magnesiothermic reduction with volume combustion synthesis and mechanochemical processing. Starting materials were pure TiO_2 powder, pure boric acid powder, and magnesium powder. Experiments were conducted both with boric acid and boric oxide (B_2O_3) obtained from calcination of boric acid, with the objective of determining the effect of calcination of boric acid on TiB_2 formation.

It was stated that, undesired secondary phases such as $3MgO.B_2O_3$ and $2MgO.TiO_2$ form during magnesiothermic production of TiB_2 [13]. Therefore, relative proportion, furnace temperature, and time were used as the experimental variables with the objective of determination of the optimum conditions to obtain a mixture of TiB_2 and MgO with no additional side products. Products were subjected to Powder X-Ray Diffraction (XRD) and Scanning Electron Microscopy (SEM) analysis to determine their nature.

The products were then subjected to acid leaching with the aim of removing MgO and any unreacted reactant from the mixture to obtain pure TiB_2. TiB_2 also dissolves and gets lost during acid leaching which decreases the efficiency [14]. To reduce TiB_2 loss, experiments were performed in order to find acid solutions of the optimum concentration. Acid concentration and leaching time were used as the experimental variables.

The outline of this thesis is given as follows: Chapter II presents previously reported studies about properties, applications and production methods of titanium diboride. In chapter III experimental set up for used techniques is summarized. Moreover, determination of ignition temperature, calcination of boric acid, and experimental procedures including ball milling and leaching processes are explained. In chapter IV, experimental results are given with discussions. Finally, the conclusions are presented in the last chapter.

CHAPTER II

LITERATURE SURVEY

2.1 Introduction

In this chapter, basic properties of titanium diboride are given starting from its crystal structure to mechanical, thermal, electrical, and chemical properties which are important in many applications. Some of these application areas of TiB_2 are given. In addition, production methods of TiB_2 are presented in detail.

2.2 General Properties

Titanium diboride is a member of borides consisting of group IV metals [15]. It crystallizes in hexagonal structure with one titanium atom at the origin of the unit cell (0, 0, 0) and two boron atoms at the side 2d (1/3, 2/3, 1/2) (Fig.2.1(a)). Its structure can be described as a stacking of hexagonal parallel boron sheets, which are perpendicular to c-axis and intercalated with a sheet consisting of titanium atoms having hexagonal symmetry [16]. There are six equidistant titanium neighbors of each titanium atom in its plane while each metal atom has 12 equidistant boron atoms, six of which in the plane above the metal atom and other six in the plane below (Fig.2.1 (b)) [2].

(a)   (b)
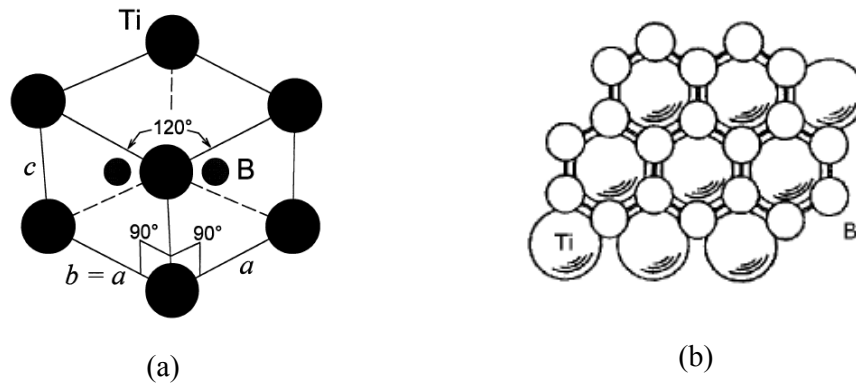
Fig.2.1 (a) The hexagonal unit cell of single crystal TiB_2, a=b≠c, α=β=90°, γ=120°
(b) Hexagonal layered TiB_2 structure

The structure of TiB_2 is composed of Ti-Ti, Ti-B and B-B bonds. Between atoms there is strong covalent bonding which gives rise to possessing extremely high melting point and high hardness [16].

The diboride of titanium has higher melting point when compared with many other diborides which are the members of the group IV, VI, and VII. Due to this unique property, TiB_2 becomes one of the most stable borides [2]. Table 2.1 indicates melting points of some transition metals and those of their diborides.

Table 2.1 Melting points of some transition metals and those of their diboride compounds [2]

Transition Metal	T_m of Metals (^{o}C)	T_m of Diborides (^{o}C)
Zr	1850	3050
Ti	1700	2920
V	1735	2400
Mo	2620	2100
Cr	1850	1900

Different temperatures exist for melting of TiB_2 in literature; it is given as 2980 ^{o}C [17-19], as 3200 ^{o}C [20] and as 2593 ^{o}C [21].

For many applications, one of the important properties which any material is desired to possess is low density. Density of titanium diboride has been theoretically calculated as 4.52 g/cm^3 [22]. In addition, R. G. Munro [23] has reported density of TiB_2 as 4.500 ($\pm$0.0032) g/cm^3. This value is lower than density of steel (7.75-8.00g/cm^3) [1] but higher than density of B_4C (2.52 g/cm^3) [24].

Diboride of titanium also has high hardness. It has the highest microhardness value among the transition metal diborides [2]. Table 2.2 illustrates microhardness of some transition metal diboride compounds, stainless steel and diamond.

Table 2.2 Microhardness of IV, V, and VI group transition metal diborides, stainless steel and diamond [2]

Boride Compounds	Microhardness (kg/mm^2)
TiB_2	3400
HfB_2	2900
TaB_2	2500
ZrB_2	2200
NbB_2	2200
VB_2	2070
CrB_2	1800
MoB_2	1200
Stainless Steel	720
Diamond	6020

In general, electrical conductivities of borides are better than those of carbides. Among the borides, TiB_2 is one of the best electrical conductors [25]. Its temperature

coefficient of electrical conductivity is negative. In addition, it shows very good thermal conductivity [26]. Moreover, its thermal expansion coefficient is very small when compared to thermal expansion coefficient of titanium. The electrical resistivities, thermal conductivities and thermal expansion coefficients of titanium diboride and some other diborides are given in Table 2.3 [25].

Table 2.3 Resistivity, thermal conductivity and thermal expansion coefficients of some diborides

Diboride Compounds	Resistivity (μohm.cm) (at 20 ^{o}C)	Thermal Conductivity (cal/cm.sec.^{o}C)	Thermal Expansion Coefficient (x 10^6 K^{-1})
TiB$_2$	9-15	0.062	6.6
ZrB$_2$	7-10	0.055	5.5
HfB$_2$	10-12	-	5.3
VB$_2$	16-38	-	15.9
NbB$_2$	12-65	0.040	8.4
TaB$_2$	14-68	0.030	5.9
CrB$_2$	21-56	-	6.7

Compared with the transition metal diborides of group V, diborides of group IV, particularly zirconium and hafnium diborides, are less stable in acid solutions. However, for diborides of group IV, chemical resistance to acids increases from hafnium diboride to titanium diboride [15]. Although chemical stability of TiB$_2$ is high, it is slightly soluble in hydrochloric acid [27]. In addition, it has been found that it is attacked by H$_2$SO$_4$ and soluble in cold HNO$_3$ [2]. Moreover, TiB$_2$ does not react with molten, nonferrous metals including Cu, Zn and Al. Due to this property; it becomes an important material for many applications [28, 29, 17].

It has been reported by Schwartz [17] that the elastic modulus of titanium diboride is ranging from 510 to 575 GPa. Königshofer et al. [30] have stated the elastic modulus calculated from two pure TiB_2 powders which have different grain sizes and different C, N, O quantities change in a small range. They found their elastic modulus as 512 and 485 GPa. Another important property of titanium diboride is its high wear resistance. This provides it to be used in several applications requiring resistance to wear even at high temperatures [9].

2.3 Applications

As it was stated previously, titanium diboride can be used for many industrial objectives such as production of protective layers in order to avoid wearing in tribological systems and as reinforcement materials in composites which are used in military applications.

TiB_2 can be used in wear resistant parts, cutting tools, and in aluminum smelting as a cathode material.

In 2000, Pfohl et al. have performed a study in order to examine mechanical properties of TiB_2 [31]. Titanium diboride was coated on hardened hot work steel by PACVD (Plasma-Assisted Chemical Vapor Deposition). In order to investigate the tribology of the coated surface, pin-on-disk test was conducted using 100Cr6 steel, aluminum and alumina pins. It was revealed that when pin materials were 100Cr6 steel and aluminum, no wear was observed; while alumina pin resulted in wear. As a result, it was stated that TiB_2 coatings could be suitable for wear resistant application involving contact with aluminum parts. Hardness properties of TiB_2 coatings were studied by R. Kullmer et al. [32]. In this investigation, TiB_2 coatings were deposited by PACVD on hot worked steel and high speed steel. Plastic hardness of TiB_2 was found as 100 GPa and Vickers Hardness was measured as 5600 $HV_{0.01}$. The study has concluded that these layers were very suitable for protective coating.

Anal et al. [5], in 2006, produced TiB_2-reinforced iron matrix composite (Fe-TiB_2) using aluminothermic reduction reaction. It was found from the wear tests that Fe-TiB_2 shows better wear resistance compared with high-chromium iron, which is a standard wear resistant material. In addition, it has been found that Fe-TiB_2 has high temperature stability.

Friction and wear behavior of TiB_2 coating which was deposited by magnetron sputtering on to high speed steel was studied by Prakashand et al. [33]. Fretting wear tests were conducted at 600 ^{o}C for 1 hour on as deposited sample and sample after annealing in air. It was revealed that as deposited sample showed better wear resistance than TiN coating. However, it was found that annealed TiB_2 coating had low wear resistance.

Augustine et al. [34] have studied reinforced ceramic coating on cutting tools. It has been reported that in order to produce composite coatings which have desired properties for cutting tool applications, ceramic matrix or ceramic whisker can be TiB_2. In addition, it was stated that to obtain sufficient reinforcement of ceramic coating, TiB_2 whisker content should be 2-40% volume percent of whiskers in ceramic composites.

Jianxin et al. [35] focused on the properties of Al_2O_3-TiB_2 ceramic tools in dry high speed machining of hardened steel. Al_2O_3/TiB_2 composite cutting tools with different TiB_2 content were prepared by hot pressing. Then, cutting tests were applied. It was observed that friction coefficient between the tool-chip interface and wear rates in dry high speed machining of hardened steel were decreased when compared with that of low speed machining. The reason of this decrease was considered as formation of self-lubricating oxide film between chip and tip of Al_2O_3/TiB_2 composite. In addition, an increase in the reduction effect was found with higher TiB_2 content.

Titanium diboride coating applied by PVD is harder than PVD TiN coatings and it also resists to aluminum [36]. Because of this, it can be used in machining of

aluminum alloy. Fig.2.2 shows machining of aluminum alloy with TiB_2 coated metal by PVD technique.

Fig.2.2 Metal tip coated with TiB_2 while machining aluminum alloy [36]

TiB_2 can be also used in electrochemical production of aluminum. During this process, sodium, which is coated on the carbon cathode of the cells used for production of aluminum, interacts with carbon. This results in swelling and cracking of the cathodes after some period of operation [37]. Therefore, it is possible to say that carbon cathodes decrease the life time of cells and increase waste cathode materials [38]. In order to overcome these problems, carbon cathodes are coated with TiB_2 when life time of the carbon cathodes increases [37, 39].

Sekhar et al. [37] have investigated some properties of porous cathode coated with titanium diboride and colloidal alumina AlO(OH) composite. Composite slurry have been prepared by mixing of TiB_2 and AlO(OH). Then, coating of carbon cathode has been performed by brushing or spraying of this mixture on the carbon. Sodium resistance test has been applied to the coated carbon cathodes and uncoated carbon

cathodes. It has been reported that coated samples show higher sodium resistance than uncoated samples. In addition, it has been stated in this research that in order to make useful coating on carbon cathode, dissolution of the coating in aluminum should be low and coating should be well wetted by aluminum.

The solubility and wettability of TiB_2 coating on carbon cathode were the subjects of the study conducted by Devyatkin et al. [39]. In this investigation, electrochemical synthesis has been used for TiB_2 coating on carbon cathode. It has been revealed that solubility of TiB_2 in molten aluminum at 1300 K is so low that it could not be measured in laboratory cells. Moreover, it has been reported that contact angle between aluminum and coating is 0°, which indicated complete wetting.

Titanium diboride can also be used for military applications [40-42]. Ti-TiB_2 composites were used for body armour [41]. Today, due to an increase in usage of the small calibre armour piercing projectile, wearers of body armour and lightly armoured combat vehicles are under threat. In order to overcome threat of small calibre projectiles, lightweight armours are designed. In 2005, Pettersson et al. [41] produced Ti-TiB_2 composites with different Ti content by spark plasma sintering (SPS). Hardness and ballistic tests were applied. Results of hardness test showed that hardness of composite with titanium content of 5-6 wt% is 25 GPa, which is 35% higher than material containing 1 wt% Ti. Ballistic tests with 7.62 AP projectile indicated that capability of protection of the SPS-$(TiB_2)_{0.95}(Ti)_{0.05}$ composite was better than that of TiB_2 produced by hot isostatic pressing (HIP).

2.4 Production Methods

In this section, preparation methods of titanium diboride and previous studies about these methods will be given. However, it is essential to give some information about self-propagating high temperature synthesis (SHS) and thermic (or thermite) reactions before the preparation methods of TiB_2.

SHS is an energy-efficient method for production of refractory ceramics. In this technique, constituent elements are mixed, compacted, and ignited with a suitable heat source [43]. The most important feature of SHS is release of sufficient heat for the self-sustaining reaction after ignition. Due to high temperatures attained in SHS processes, it is expected that purity of final product is better than reactant mixture [44] due to evaporation of impurities. SHS reaction can be started by many techniques. The most commonly used one is ignition by the help of a tungsten wire. This ignitor is connected to compacted reactant mixture in order to ignite mixture directly by heating with electrical discharge [45].

Thermite reaction is an oxidation-reduction reaction where a metallic reducing agent reacts with metallic or non-metallic oxide and form more stable oxide and corresponding metal or non-metal of the reactant oxide. This type of reactions are written in generally as following

$$R + XO = RO + X + \Delta H \tag{2.1}$$

where R is a reducing agent, X is a metal or a non-metal, RO and XO are the corresponding oxides, and ΔH heat generated by the reaction.

Thermite reactions are strongly exothermic and once start become self-sustaining. This makes thermite reactions extremely energy efficient.

Thermite powders require very simple reactor and minimal energy. On the other hand, they need a leaching step in order to remove undesired oxide part [27].

All metal reducing agents have negative Gibbs free energies of oxide formation. However, in order to select a good reducing agent, it is important to consider that oxide of the reducing agent whose Gibbs free energy is the most negative is the best choice due to its property of most stable oxide. In Fig.2.3, Gibbs free energies for formation of some common reducing agent oxides are shown.

12
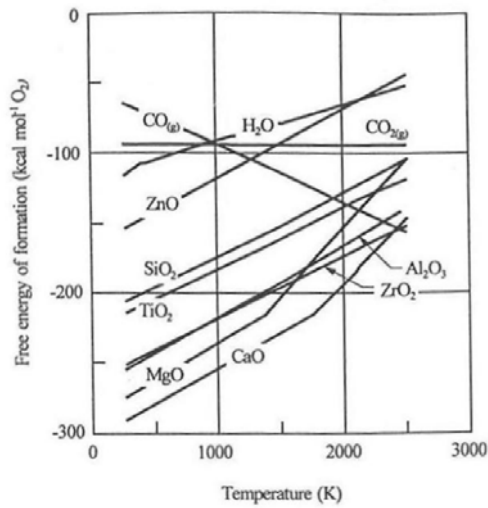
Fig.2.3 Gibbs free energies of formation for oxides

As it is seen from Fig.2.3, both magnesium oxide and calcium oxide have more negative Gibbs free energies than the others. In this study, magnesium was used as the reducing agent due to high cost and difficulties in handling of metallic calcium [46].

Titanium diboride, which is one of the diborides of IV group transition metals, can be produced in five different ways. These are listed as follows [2, 25, 15, 47-50]:

- Solid state reaction between titanium and boron
- Reduction of oxides (TiO_2 and B_2O_3)
    - by carbon (carbothermic reduction method) and boron carbide
    - by aluminum (aluminothermic reduction method)
    - by magnesium (magnesiothermic reduction method)
- Electrolysis of molten salts
- Vapor phase deposition
- Mechanochemical synthesis or mechanochemical processing

Since in this study magnesium was used as the metal reducing agent, methods of oxide reduction in general and magnesiothermic reduction in particular are given in detail. In addition, TiB_2 was also produced by mechanochemical synthesis using a ball-mill; therefore, mechanochemical synthesis is also given in detail. Other production methods are described briefly.

2.4.1 Solid State Reaction between Titanium and Boron

Reaction between titanium and elemental boron is the most direct method of producing of titanium diboride in the powdered form. Production of TiB_2 by using this process enables formation of high purity product and control of its composition [50]. Using this method, small amounts of products with high purity are obtained. Although the technique including reaction between Ti and B has advantages some of which were given above, it has also some disadvantages. For example, elemental powder of Ti is very reactive with oxygen. Therefore, individual Ti powder particles can be covered by oxide film immediately. In addition, reaction between Ti and B is so violently exothermic that powders may cause very dangerous fires. In order to overcome these disadvantages, instead of using powders of elemental boron and titanium, their oxides are preferred [25]. According to literature survey done, few articles have been found about solid state reaction between titanium and boron. These studies can be summarized as follows:

Roy et al. [11] have studied the production of TiB_2 by combustion synthesis under vacuum and has not observed unreacted Ti and B in the product after SHS of Ti and B compact. This has been explained with completeness of the Ti+2B reaction. It has been also indicated that sponge-like structure was obtained after the reaction.

Holt et al. [51] have focused on combustion of crystalline and amorphous titanium and boron powders. They have prepared pellets containing stoichiometric amount of Ti and B by cold pressing and ignited by using SHS technique. Activation energy of the Ti + 2B=TiB_2 reaction has been found as 539 kJ and activation energy of

sintering of TiB_2 has been calculated as 773 kJ. Because the activation energy of Ti + 2B reaction is lower than that of sintering of TiB_2, it has been suggested that sintering and combustion of TiB_2 did not occur by the same mechanism.

2.4.2 Reduction of TiO_2 and B_2O_3 by Carbon (Carbothermic Reduction Method) and Boron Carbide

The most common reduction material for metal oxides is carbon [2]. Although contamination is a big problem for production of pure materials, it can not be taken into consideration when carbon is used as a reducing agent because its quantity will be very small in the product (in the order of between 0.05 and 0.02%) [2]. However, boron carbide results in highly contaminated materials [15].

A detailed study about carbothermic reaction has been performed by Kim et al. [52]. It has been reported in this investigation that carbothermic formation of TiB_2 can be described by two different chemical reactions. These are;

$$TiO_2 + 1/2\ B_4C + 3/2C = TiB_2 + 2\ CO \qquad\qquad (2.2)$$

$$TiO_2 + B_2O_3 + 5C = TiB_2 + 5CO \qquad . \qquad (2.3)$$

Reaction (2.2) and (2.3) are very similar to each other. The differences between these two are the starting materials and amount of resulting CO. Generally, Reaction (2.2) is the more commonly used carbothermic reduction method due to absence of low melting point of B_2O_3 [52].

Kim et al. [52] in this study have prepared a pellet containing TiO_2-B_4C-C stoichiometric mixture and this charge has been preheated slowly to 1400 ^{o}C and then heated rapidly to 2000 ^{o}C under argon atmosphere so as to start carbothermic reaction. In order to prevent oxidation of the product, it was cooled in the furnace below red heat. After cooling, small crystallites were obtained. In addition, it has

been reported that purity of the produced TiB_2 powders were >98% and they were slightly boron rich. Moreover, milling of product powder has been studied and it has been found that after milling of TiB_2 powder, pressureless sinterable powder was obtained [52].

Krishnarao et al. [53] investigated formation of TiB_2 whiskers through carbothermic reduction method. In order to facilitate formation of TiB_2 whiskers, K_2CO_3 and $NiCl_2$ solutions were used. TiO_2 and $NiCl_2$ solutions were mixed and then K_2CO_3 solution was added and stirred. After that, this mixture was dried in the oven at 110 ^{o}C. B_2O_3 and C were added to the dry mixture. This mixture was ignited in the high temperature furnace under argon atmosphere. It was observed that whisker formation took place at low temperatures (940-1200 ^{o}C). They also studied the effect of TiO_2 content on the resulting product. It was revealed that decreasing TiO_2 to 0.5 mole content caused only TiB_2 formation while further decreasing to 0.25 mole gave rise to synthesis of B_4C apart from TiB_2 [53].

Synthesis of TiB_2 by reduction of carbon coated TiO_2 mixed with B_4C was the subject of a research conducted by Koc et al. [54]. In this study, it was reported that carbon coated TiO_2 precursors containing B_4C could be used in production of high quality TiB_2 powders.

Greenhouse et al. [55] and Nelson et al. [56] have studied the high temperature reaction between TiC and B_4C. TiC and B_4C heated under argon atmosphere were found to react at temperature above 1920 ^{o}C according to:

$$2TiC + B_4C = 2TiB_2 + 3C \qquad . \qquad (2.4)$$

2.4.3 Reduction of TiO_2 and B_2O_3 by Aluminum (Aluminothermic Reduction Method)

Aluminothermic production is one of the classic titanium diboride production methods in which TiO_2 and B_2O_3 are reduced by aluminum. Due to low cost of aluminum, reduction by Al is the most cost effective method [25]. Below, studies about TiB_2 production using aluminothermic reduction method are given.

One of the first studies about production of TiB_2 by aluminothermic reduction was performed by Logan et al. [7], in 1988. Production of TiB_2 was performed by the following reaction;

$$3TiO_2 + 3B_2O_3 + 10Al = 5Al_2O_3 + 3TiB_2 \qquad . \qquad (2.5)$$

In this investigation, it was reported that the ignition temperature decreased by decreasing particle size of Al. It was also stated that the product obtained by ignition in air-atmosphere did not contain any TiN. In addition, TiB_2 and Al_2O_3 could be distinguished only in microscopic scale.

Taneoka et al. [57] produced TiB_2 by reaction between titanium, boron and aluminum under vacuum. They observed that all Al was vaporized and only TiB_2 was obtained as the final product. This evaporation was explained as self-purification behavior of combustion synthesis.

Kurtoğlu [58] and Elmadağlı [59] studied the production of Al_2O_3-TiB_2-reinforced aluminum metal matrix composite. TiB_2 powders used in these studies were obtained by aluminothermic reduction. It was also concluded that H_3BO_3 could be used instead of B_2O_3 during TiB_2 production [58].

2.4.4 Reduction of TiO_2 and B_2O_3 by Magnesium (Magnesiothermic Reduction Method)

In addition to aluminum, magnesium can also be used as a reducing agent. Since it is possible to obtain pure TiB_2 by leaching of resulting magnesium oxide with dilute hydrochloric acid, magnesium is more commonly used [27].

Markovski et al. [60] studied magnesiothermic production of TiB_2, VB, VB_2, NbB, NbB_2, TaB, TaB_2, W_2B_5, Mo_2B_5, CrB_2, CrB, CaB_6, BaB_6, LaB_6, EuB_6, GdB_6 and SrB_6 and they concluded that reduction reaction by magnesium for preparation of diborides takes place by the following reaction:

$$X_nO_m + nB_2O_3 + (m+3n)\ Mg = n\ XB_2 + (m+3n)\ MgO \qquad (2.6)$$
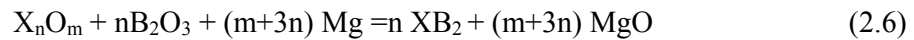
where X is the transition metal of groups II, III, and IV in the periodic table [60].

In this study, it was stated that reduction in this reaction was not a single step reduction. Reduction by magnesium for preparation of diborides takes place by the following steps. Firstly, metallic magnesium reduces boron oxide and metal oxide to free boron and metal, respectively. Then, metal and boron react with each other to form metal boride.

After reduction Reaction (2.6), in order to remove magnesium oxide from resulting product, metal boride-magnesium oxide mixture was leached in a suitable solvent. This solvent should dissolve magnesium oxide while not reacting with metal boride [60].

Logan et al. [61, 62] have focused on the production of submicron titanium diboride by magnesiothermic reduction according to reaction given below;

$$TiO_2 + B_2O_3 + 5Mg = TiB_2 + 5MgO \qquad . \qquad (2.7)$$

Magnesium borate ($Mg_3B_2O_6$) and magnesium titanate (Mg_2TiO_4) were observed to be present as minor phases in addition to the expected TiB_2 and MgO phases on the X- Ray Diffraction (XRD) pattern of reaction products. The amounts of the minor phases magnesium borate and magnesium titanate were found to be affected by use of excess amounts of B_2O_3 and Mg. These authors studied elimination of MgO, $Mg_3B_2O_6$ and Mg_2TiO_4 from the reaction products by leaching. The best result was obtained in leaching of reaction products at 90 ^{o}C in nitric acid solution having pH between 2.5 and 4 [61]. HCl leaching is preferred to HNO_3 leaching; however, TiB_2 is more soluble in HNO_3 than in HCl [27].

Sundaram et al. [63] also investigated production of TiB_2 according to the overall Reaction (2.7). They suggested titanium resulting from reduction of TiO_2 by Mg according to the reaction

$$2Mg + TiO_2 = 2MgO + Ti \qquad (2.8)$$

To react with B_2O_3 according to the reaction:

$$5Ti + 2B_2O_3 = 2TiB_2 + 3TiO_2 \qquad (2.9)$$

to form TiB_2.

They reported formation of Mg_2TiO_4 and $Mg_3B_2O_6$ minor phases. In order to study formation of Mg_2TiO_4 minor phase, Reaction (2.8) was performed under air and argon atmosphere. This reaction was found to start at 592 ^{o}C under air when Mg_2TiO_4 was found to have formed in addition to MgO. It was observed that the same mixture did not form Mg_2TiO_4 under argon atmosphere. It was reported that the only products formed under argon atmosphere were MgO and Ti. Mg_2TiO_4 was concluded to form by reaction of Mg, TiO_2 and O_2 in the atmosphere according to:

$$2Mg + O_2 + TiO_2 = Mg_2TiO_4 \qquad (2.10)$$

19

or reaction between magnesium oxide and titanium oxide according to:

$$2MgO + TiO_2 = Mg_2TiO_4 \qquad (2.11)$$

Similarly, in order to find out formation reaction of $Mg_3B_2O_6$ according to reaction,

$$3Mg + B_2O_3 = 3MgO + 2B \qquad (2.12)$$
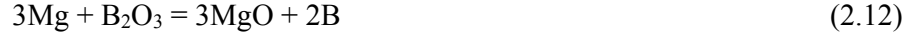
$3Mg$-B_2O_3 mixture was ignited in air and argon atmosphere [63]. No reaction was observed to have taken place under argon atmosphere, although thermodynamically the reaction was expected. However, under air atmosphere reaction between Mg and B_2O_3 was observed at 629 $^{\circ}$C and $Mg_3B_2O_6$ and MgO formed. $Mg_3B_2O_6$ was suggested to form with reaction between Mg, O_2 in the atmosphere and B_2O_3 according to Reaction (2.13) or reaction between MgO and B_2O_3 according to Reaction (2.14) [63].

$$3Mg + 3/2\ O_2 + B_2O_3 = Mg_3B_2O_6 \qquad (2.13)$$

$$3MgO + B_2O_3 = Mg_3B_2O_6 \qquad (2.14)$$
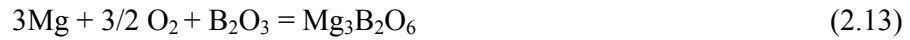
Sundaram et al. [13] in a later study on formation of TiB_2 by magnesium reduction of TiO_2 and B_2O_3 concluded magnesium to reduce TiO_2 and B_2O_3 to form Ti and MgB_2 according to Reaction (2.15) and

$$4Mg + B_2O_3 = 3MgO + MgB_2 \qquad (2.15)$$

which in turn reacted according to the reaction

$$Ti + MgB_2 = TiB_2 + Mg \qquad (2.16)$$

to form TiB_2.

$Mg_2B_2O_5$ in addition to Mg_2TiO_4 and $Mg_3B_2O_6$ minor phases was also observed to form in this study.

Weimin et al. [64] studied reaction processes in the B_2O_3-TiO_2-Mg system. In this research, experiments were conducted under argon atmosphere. The results obtained were similar to those obtained by Sundaram et al. [13, 63].

Production of nanometric TiB_2 by magnesiothermic reduction by ball milling and leaching of the resulting MgO and TiB_2 mixture was reported by Welham [65]. In this investigation, 1 M HCl solution was chosen as leachant and leaching was performed for 2 hours at room temperature at 1% (1/100(gram/cc)) slurry density. XRD pattern of the leached sample indicated only TiB_2 peaks which indicated that MgO could be removed from the mixture. Some dissolution of TiB_2 in 1M HCl also was observed.

Ricceri et al. [66] studied TiB_2 formation by mechanosynthesis of TiO_2, B_2O_3, and Mg reactants and leaching of MgO-TiB_2 mixture. The resulting ball milled product was leached for 2 hours in 0.5 M HCl at 1% slurry density at room temperature in order to remove MgO, unreacted Mg and Fe coming from balls. It was observed that leached powder contained only TiB_2. In addition, this leached powder had larger crystal size than the unleached one. This was an unexpected result in view of partial dissolution of TiB_2 during leaching.

Demircan et al. [14] conducted a study on separation of MgO from MgO-TiB_2 mixtures by HCl leaching. Leaching experiments were performed with 1/5 solid/liquid ratio at 293 K with HCl solutions of concentration varying from 0 to 9.3 M. Temperature of the system was observed to increase during leaching due to leaching of MgO by HCl being exothermic. Rise of temperature of the system was found to increase with increase in HCl concentration. In order to compensate for

evaporation of acid solution due to high temperature, additional acid solution was made gradually during leaching. XRD pattern of the leached samples showed that intensities of the MgO peaks decreased while intensities of the TiB_2 peaks increased with increase in HCl concentration. XRD pattern of the sample leached with leaching using 9.3 M HCl indicated no traces of MgO or minor phases and was similar to XRD pattern of commercial TiB_2 [14].

Merzhanov [27] stated that magnesium boride may also form in magnesiothermic reduction of TiO_2-B_2O_3 mixtures and that unreacted titanium, boron, boric oxide and magnesium may exist in reaction product. The optimum condition in order to form only TiB_2 phase is given in TiO_2, B_2O_3, and Mg diagram in Fig.2.4.
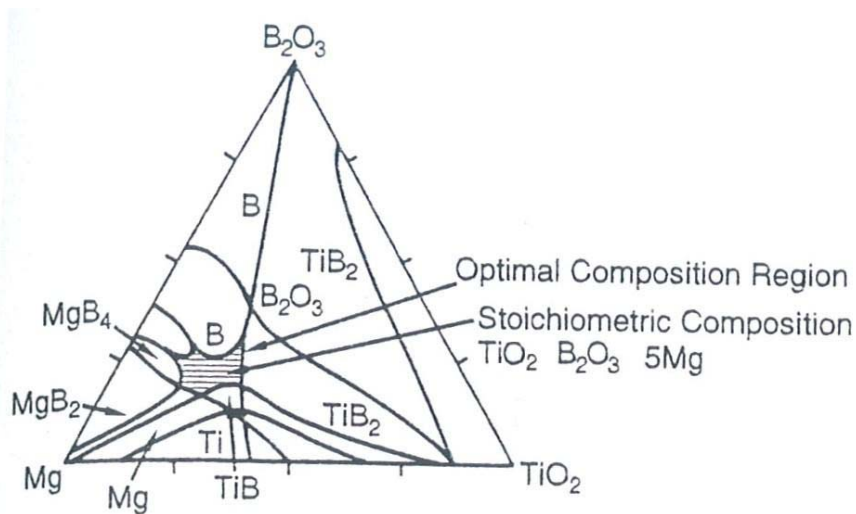
Fig.2.4 Diagram showing possible phases which can form in the system of TiO_2-B_2O_3-Mg [27]

2.4.5 Electrolysis of Molten Salts

Different boride compounds such as ZrB_2, TiB_2, TaB_2, YbB_6, and SrB_6 can be synthesized electrochemically from molten salts [67-70]. This technique enables production of smooth single crystal coatings even at surfaces having complicated geometry and controlling the composition of the deposited layers [67]. Titanium diboride can be coated by using different electrolyte solutions given such as NaCl-KCl-$TiCl_3$-KBF_4, LiF-KF-B_2O_3-TiO_2 and KCl-KF-K_2TiF_6-KBF_4 [67].

It is possible to coat titanium diboride containing 30.8% - 31.2% B and 68.5% - 69.1% Ti, using bath of the composition $1/2TiO_2 + 2B_2O_3 + MgO + MgF_2$ at about $1000\ ^oC$ [15].

2.4.6 Deposition from Vapor Phase

Vapor phase deposition is a method used for depositing coatings of refractory materials at temperatures below their melting points. This technique enables to deposit layers having thickness of less than a micron to several millimeters depending on the plating time [71].

Vapor phase deposition of refractory materials like TiB_2, ZrB_2, VB_2, HfB_2, and MoB_2 was investigated by Campbell et al. as early as 1949 [71]. He focused on coating characteristics, rate of deposition, efficiency of vapor phase reactions, and uniformity of coating. It was reported that titanium diboride was deposited at temperatures between 1000 and 1300 ^oC and 1 atm pressure by hydrogen reduction of titanium tetrachloride and boron trichloride according to the reaction:

$$TiCl_4 + 2BCl_3 + 5H_2 = TiB_2 + 10HCl \qquad . \qquad\qquad (2.17)$$

Since Reaction (2.17) is highly exothermic, the solid nuclei grow fast at the temperature they are formed. Hence, small size TiB_2 production may become

impossible by hydrogen reduction reaction [71]. In order to solve this problem, Brynestad et al. [72] studied formation of TiB_2 from titanium trichloride and boron trichloride according to the reaction:

$$10 \text{ TiCl}_3 \text{ (g)} + 2 \text{ BCl}_3 \text{ (g)} = \text{TiB}_2 \text{ (s)} + 9 \text{ TiCl}_4 \text{ (g)} \quad \approx 1500 \text{ K} \qquad (2.18)$$
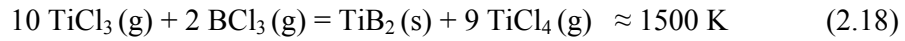
and succeeded to prepare submicron TiB_2.

2.4.7 Mechanochemical Synthesis

Mechanochemical synthesis (or mechanosynthesis or mechanochemical processing (MCP)) is the term applied to the powder process in which chemical reactions and phase transformations take place due to application of mechanical energy [73]. It is used in synthesis of many systems such as metal alloys and ceramics [66].

Mechanochemical processing is used for oxidation-reduction reactions, exchange reactions, decomposition of compounds and phase transformations. Mechanical energy converted into chemical energy is the cause of chemical reactions in MCP. It involves repeated welding, fracturing, and rewelding of a mixture of powder particles to produce an extremely fine microstructure. Generally, mechanochemical synthesis is made in high-energy ball mills [73].

Reaction used in mechanochemical synthesis is similar to reaction used in reduction.

$$R + XO = RO + X + \Delta H \qquad (2.19)$$

where R is a reducing agent, X is a metal or a non-metal, RO and XO are the corresponding oxides, and ΔH is heat generated by the reaction.

Reaction rate is very low for Reaction (2.19) at low temperatures. Therefore, in order to achieve reasonable reaction rates, elevated temperatures are necessary. MCP may

provide increase in kinetics of the reaction without the necessity of elevated temperatures. During MCP, repeated cold welding and fracture of the reactant powder cause an increase in area of the contact between powder particles which lead to an increase in the reaction rate. Thus, reactions normally requiring high temperatures can take place at low temperatures [73].

Two different reaction kinetics are possible in mechanochemical synthesis:

a) Due to increase in area of contact between powder particles, Reaction (2.19) may take place at very small volume during each collision, bringing about a gradual transformation, or

b) SHS reaction may be started if enthalpy of Reaction (2.19) is sufficiently high.

Combustion occurs during MCP when contact between the reactant powders is intimate. Intimate contact is an important requirement to obtain faster reaction rate during the process. This can be achieved during milling of ductile and brittle systems because brittle oxides such as TiO_2 and B_2O_3 are dispersed in the ductile matrix such as Mg.

During conventional SHS, heat loss to the surrounding is very low. However, during MCP, powders are in very close contact with the milling tools and this causes relatively high heat loss. As a result of this, conventional SHS which can normally occur for a given system may not be possible during MCP [73].

Welham milled boron oxide, titanium oxide and magnesium powder and found the reaction to be complete after milling between 10-15 hours by ball milling with planetary ball mill. As a result, only TiB_2 and MgO phases were obtained and MgO was removed after acid leaching [74].

Mechanosynthesis of TiB_2 from titanium oxide, boron oxide and magnesium was studied by R. Ricceri et al. [66]. In this study ball milling was performed for 2 hours

in vibratory ball mill. Resulting MgO and TiB_2 mixtures were leached in 0.5M HCl solution for 2 hours and it was reported that TiB_2 was obtained with molar yield of 81%.

Hwang et al. [75] studied mechanochemical synthesis of TiB_2 by milling of Ti and B powders in a planetary ball mill under argon atmosphere. TiB_2 peaks were observed to appear after 180 hours of ball milling and Ti peaks were not observed after 280 hours of milling indicating the reaction to be complete in 280 hours.

CHAPTER III

EXPERIMENTAL

3.1 Introduction

In this chapter, techniques used during the study will be given and experimental set-up and procedure will be described. First, procedure for calcination of boric acid will be given. Then, preparation of reactants, ignition in the furnace and experimental set-up for determination of ignition temperature will be explained. In addition, ball milling and leaching processes will be given in detail.

3.2 Calcination of Boric Acid

In order to produce boric oxide, boric acid was calcined. This process was performed in a 90.0 mm diameter, 90.0 mm height stainless steel crucible. About 30 g of boric acid was charged into this crucible and it was placed at the center of a pot furnace. Then, the furnace was heated to 900 $^{\circ}$C and the crucible was kept at this temperature for 45 minutes. After calcination, molten boric oxide was obtained in the stainless steel crucible. This molten boric oxide was poured onto a stainless steel plate. After cooling of boric oxide, it separated from the plate easily. Then, this boric oxide was crushed using a hammer first so as to get small pieces and in order to obtain powder boric oxide, it was ground in a ceramic mortar and pestle.

3.3 Preparation of Reactant Mixture

Firstly, reactants whose purities and particle sizes are given in Table 3.1 were weighed in amounts predetermined according to Reaction (3.1) or (3.2) changing with the use of B_2O_3 or H_3BO_3, respectively. For ignition experiments, 10 g of samples were prepared. Sample ball milled for 15 hours was prepared as 25 g while sample to be ball milled for 5 hours was prepared about 20 g. Then, these powders were poured into a ceramic mortar and mixed for about 10 minutes using mortar and pestle.

$$TiO_2 + B_2O_3 + 5Mg = TiB_2 + 5MgO \tag{3.1}$$

$$TiO_2 + 2H_3BO_3 + 5Mg = TiB_2 + 5MgO + 3 H_2O \text{ (vaporized)} \tag{3.2}$$
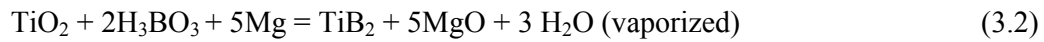
Table 3.1 Purities and particle sizes of used powders

Powder	Purity	Particle Size (μm)	Company
TiO_2	>99%	Not specified	Merck
H_3BO_3	>99.8%	Not specified	Merck
Mg	>99%	< 300 μm	Aldrich

SEM micrographs of Mg and TiO_2 powders used in the experiments are given in Fig.3.1. Magnesium powder, specified to have a particle size <300 μm by the supplier, is seen to be finer from Fig.3.1(a). Particle size of TiO_2 was determined from SEM examination to be < 0.5 μm.

<div align="center">(a)   (b)</div>
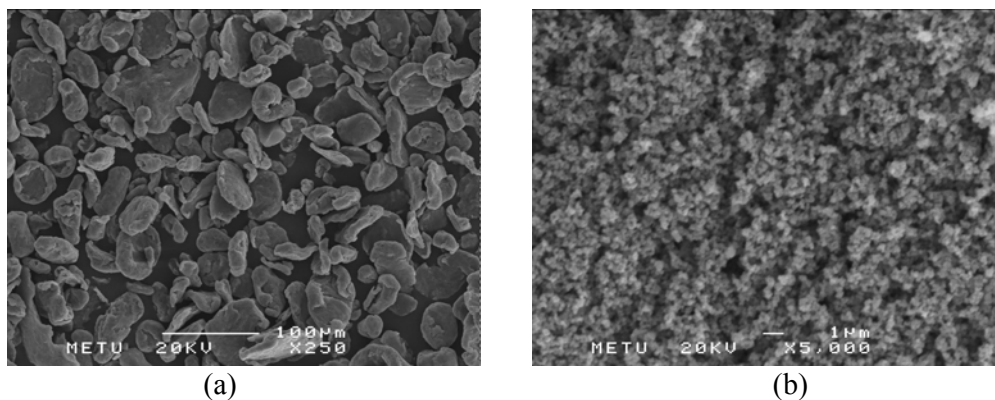
Fig.3.1 SEM micrographs of (a) Mg powder bought from Aldrich, (b) TiO_2 powder

3.4 Ignition Experiments and Determination of the Ignition Temperature

Experiments were performed in a pot furnace under air and argon atmosphere. The pot furnace used is schematically shown in Fig.3.2. The furnace was heated by kanthal resistance wire and it was connected to Gemo PC 107 temperature controller system which kept the temperature of the furnace constant with an accuracy of $\pm$ 5°C. A K type thermocouple in an alumina protection tube was used for measuring the furnace temperature. Prepared reactants mixture was put into a 90.0 mm high graphite crucible having an inside diameter of 50.0 mm and an outside diameter of 60.0 mm. Then, the lid of the crucible was closed. This crucible was placed into the preheated pot furnace having an inside diameter of 128.0 mm and depth of 136.0 mm, and the lid of the furnace was closed. Then, sufficient time was allowed for the reaction to take place in the furnace. Later, crucible was taken out and it was left for cooling in air.
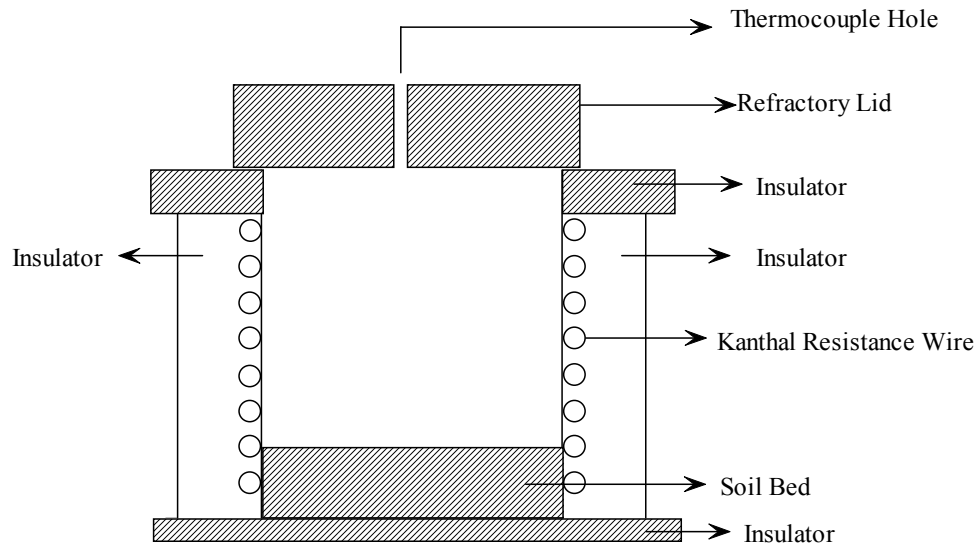
Fig.3.2 Pot furnace used during experiments.

In order to determine ignition temperature of the Reactions (3.1) and (3.2), a hole was drilled on the lid of the crucible and a K type thermocouple in an inconel protection tube was inserted into the graphite crucible. It was ensured that the thermocouple was in touch with the reactants. Then, the crucible with the thermocouple inside was placed into the preheated pot furnace and experiments were conducted. Thermocouple inside the crucible was connected to a Tetcis PC 990 temperature controller system which was linked to a computer; by using Opik 04 program, temperature and time data were recorded automatically on the computer at a frequency of 1 second. Due to sudden increase in temperature when ignition occurred, ignition temperature was determined easily using these data. The set-up used for determination of ignition temperature is schematically shown in Fig.3.3.

In some ignition experiments, argon supplied from Habaş A.Ş. with 99.998 % purity was blown to the system. In order to attain this, one additional hole was drilled to the lid of the crucible. After powder mixture was charged into the crucible, the lid was closed. Then, argon was blown into the crucible for 10 minutes with flow rate of approximately 400 cc/min., before placing the crucible into the furnace. Then, the

crucible with its content was placed into the preheated furnace. Meanwhile, argon flow was continued. During heating of the crucible in the furnace, flow rate was still kept constant at 400 cc/min. After the ignition of the reactants took place, the crucible was taken out and left for cooling under the flow of argon. Experimental set-up used for ignition under argon atmosphere is given in Fig.3.4.
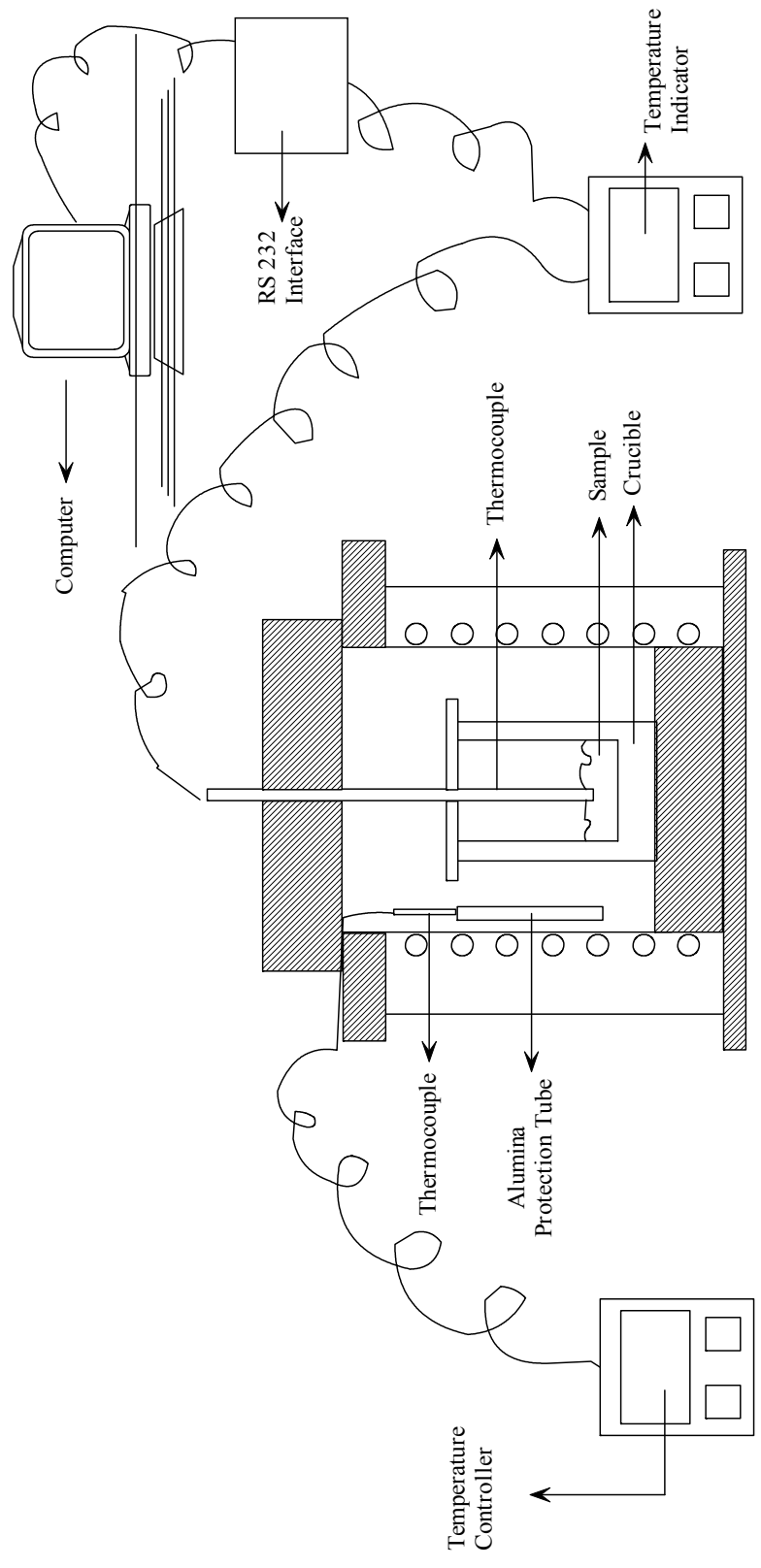
Fig.3.3 Experimental set-up used to determine ignition temperature of the sample

Computer

RS 232
Interface

Temperature
Indicator

Thermocouple

Sample

Crucible

Alumina
Pipe

Thermocouple

Alumina
Protection Tube

Flow Meter

Separator for
Overflow

Overflow
Exit

Argon Gas
Cylinder

Temperature
Controller
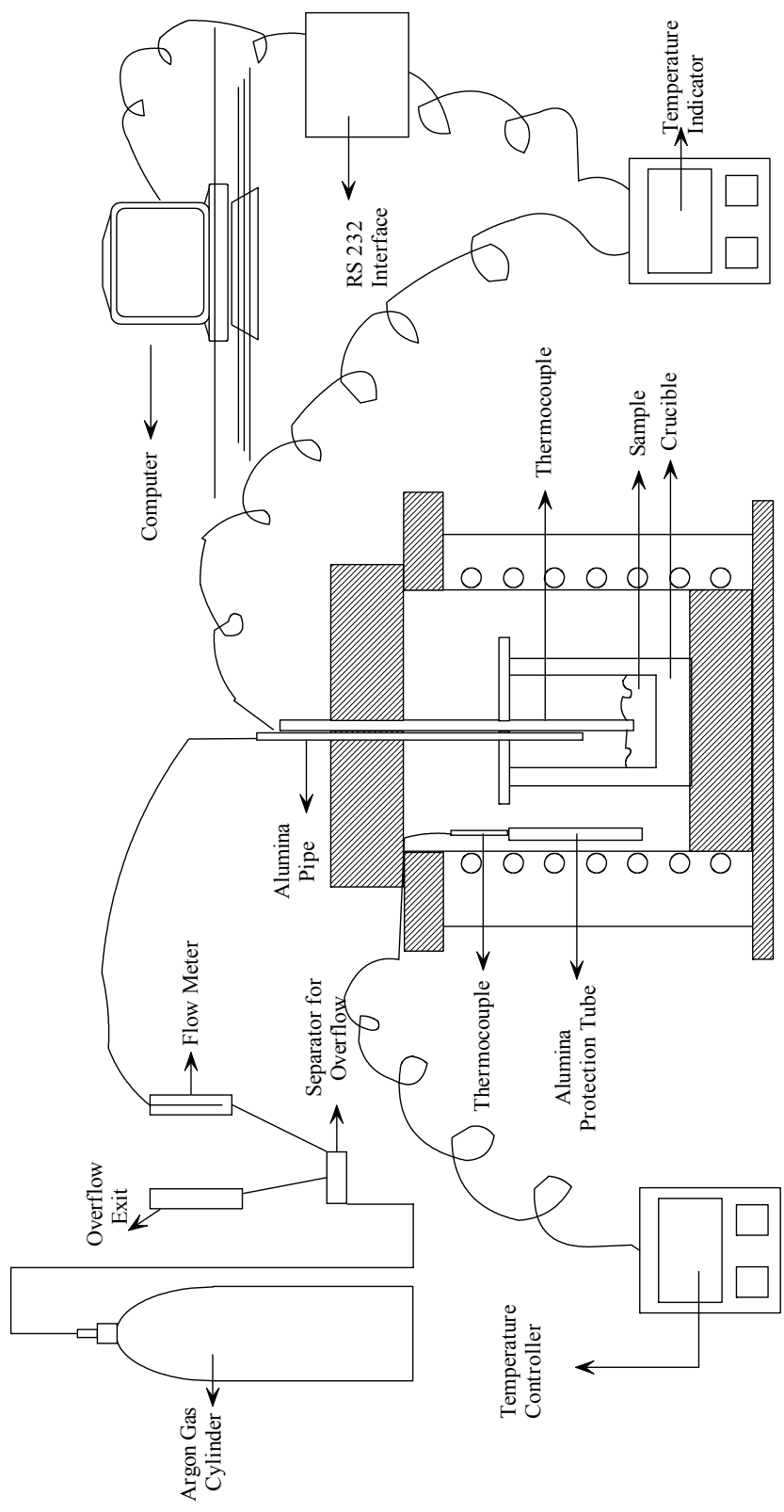
Fig.3.4 Experimental set-up used for ignition of the sample under argon atmosphere

33

3.5 Ball Milling

Ball milling process is performed in a stainless steel bowl, into which the material to be ground is placed with balls that are made of the same material as the bowl. The interaction between the balls, particles and the bowl wall result in grinding of the material.

In this study, for ball milling process a Retsch PM 100 planetary ball mill machine which can be operated with a speed between 100 and 650 rpm (rotations per minute) shown in Fig.3.5 was used [76].
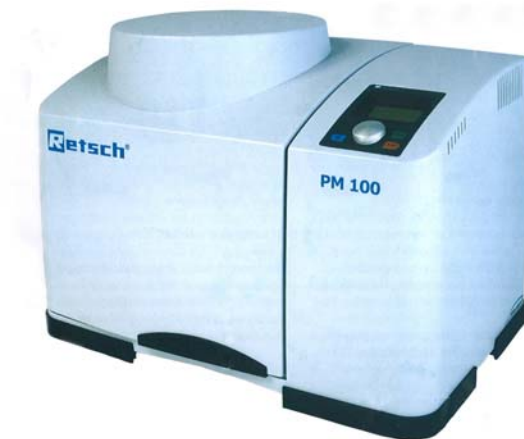
Fig.3.5 Retsch PM 100 planetary ball mill machine [76]

The principle of working of planetary ball mills is as follows: The bowl is placed on a supporting disk and the disk and the bowl are rotated around their own axes in opposite directions. The centrifugal force resulting from the rotation of the bowl around its own axis and around the support disk causes the balls to move inside the bowl. This gives rise to friction force between balls, powder, and wall of the grinding bowl. As a result, material is ground. In addition to friction, there is an impact force

produced due to the fact that grinding balls lift off and move freely through the inner chamber of the bowl and collide with the opposite inside wall. Motion of balls is schematically shown in Fig.3.6 [73].
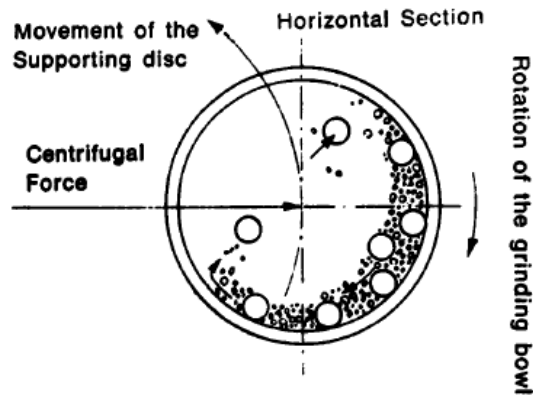
Fig.3.6 Ball motions in the planetary ball milling machine [73]

Ball milling can be used for several purposes. In the following, only two commonly used ones, which are also utilized in this study, namely mechanochemical processing and mechanical grinding will be given. If phase transformation and chemical reactions take place between particles of the powders during the milling process, the process is called Mechanochemical Processing (MCP). In addition, ball milling can be used for reduction of particle size and an increase in their surface area, this process is known as Mechanical Milling (MM) or Mechanical Grinding (MG). Although in MCP process particles in the bowl should go into reaction with each other during ball milling, in MM process no reaction takes place between the particles of the material [73]. In the present study, ball milling was used to achieve both of the aims given above. It was used to reduce the particle size before leaching and also to synthesize TiB_2 phase during milling.

Although one of the aims of milling process is to reduce the particle size, powder particles may come together due to agglomeration. This reduces the efficiency of ball milling in terms of particle size reduction. In order to prevent agglomeration effect and produce finer powders, process control agents (PCAs) may be added to the bowl before grinding. They can be solid, liquid and gas. In the present study, liquid process control agent was used. Ethanol (C_2H_5OH) was selected as the liquid medium because it is not reactive with the powders charged into the bowl.

3.5.1 Ball Milling Process for Size Reduction

Ball milling experiments performed for size reduction were made in dry condition and in ethanol medium. Ball milling parameters, ball milling medium, sizes and quantities of balls, atmosphere, ball milling rate and duration used, are given in Table 3.2.

Table 3.2 Experimental parameters used in ball milling for particle size reduction

Ball Milling For Particle Size Reduction	Meduim	Sequence	Atmosphere	Size and quantities of balls	Ball Milling Rate (rpm)	Ball Milling Duration (hour)
	Dry Ball Milling	After Ignition	Air	50 pieces with 10mm diameter	150	7
	Ethanol Ball Milling	After Ignition	Air	50 pieces with 10mm diameter	150	7

Dry ball milling was conducted as follows. Firstly, balls were placed into the grinding bowl. Then, sample was loaded into the bowl and its lid was closed. Secondly, safety closure device was closed and its screws were tightened, then the bowl was weighed. Thirdly, the bowl loaded with balls and sample was placed into the planetary ball milling machine and clamps were tightened. Weight of the bowl was adjusted for balance by tuning of a counterweight [76] (Fig.3.7). Finally, the

machine was operated with a set program. At the end of the process, the bowl was opened and the sample was taken out from the bowl. Some amount of sample was observed to be covered around the balls and also on the wall of the bowl. Ball milling machine was operated for 15 minutes at 150 rpm to have the powder covered on the wall of the bowl and the balls to be detached. This process was repeated twice. Sample detached from the bowl and the balls was then removed from the system.
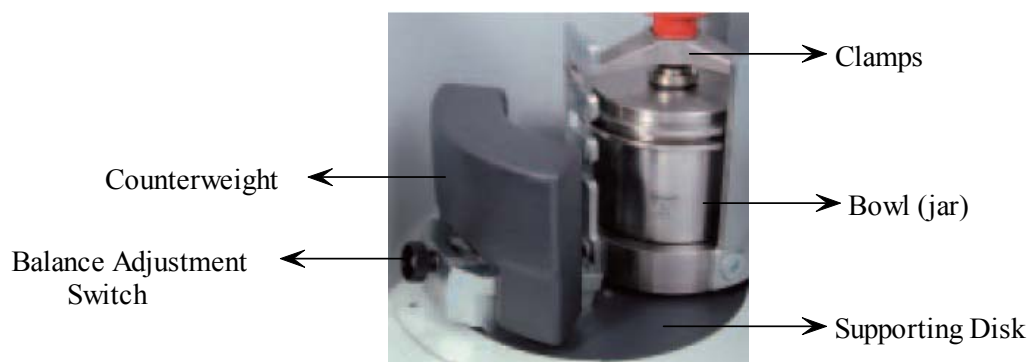
Fig.3.7 Balance adjustment [76]

In the ball milling with the ethanol medium, after loading of balls and sample into the bowl, about 40 ml ethanol, purity of which was 99.9%, was poured into the bowl and the same procedure used in dry ball milling was performed until the bowl was taken out of the milling machine. Then, lid of the bowl was opened; balls and ethanol-sample mixture were separated by passing through 4 meshes of sieve under which there was a stainless steel pan used so as to collect the ethanol-sample mixture. This is shown in Fig.3.8. The bowl, bottom of the lid, and the balls were cleaned with ethanol so as to take out the remaining sample covered on the surfaces of them. Although these were then cleaned with ethanol, some sample remained on the surface of the balls and on the inside wall of the bowl. Therefore, in order to take the remaining part, balls were charged into the bowl again and ball milling machine was operated for 15 minutes with a speed of 150 rpm in ethanol medium. This

milling was repeated twice. Then, ethanol-sample mixture and balls were passed through the sieve. The balls, the bowl and bottom of the lid were cleaned with ethanol again. Finally, ethanol-sample mixture which had been collected on the pan was dried at 70 ^{o}C in a drying oven for a period of at least 2 hours. Drying time of the mixture changed with volume of the ethanol.
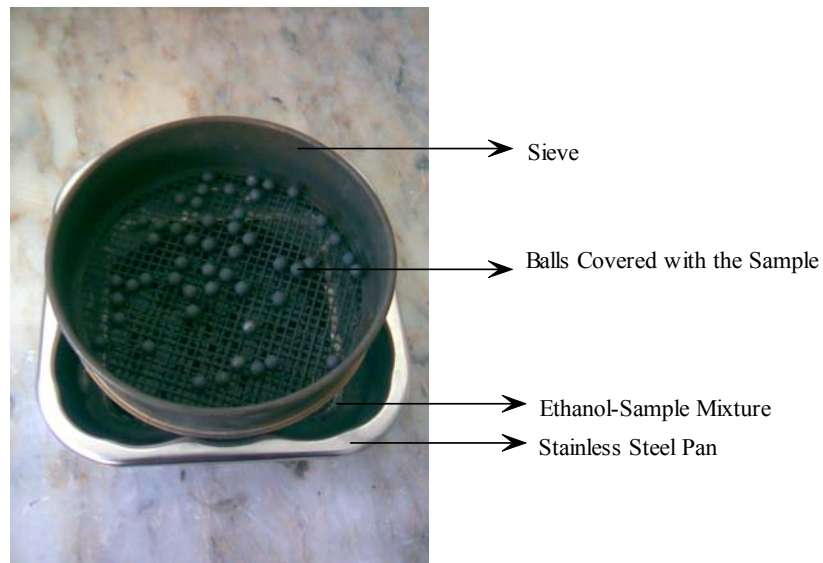
Fig.3.8 Sieve, pan, and balls after ethanol ball milling

3.5.2 Ball Milling Process for Mechanochemical Synthesis

Experiments in which ball milling was used for MCP were conducted under dry conditions in argon atmosphere. Procedure used for this type of ball milling process was similar to the procedure used in dry ball milling for particle size reduction. The only difference was that argon supplied from Habaş A.Ş. with 99.998 % purity was blown into the bowl in MCP experiments. In order to fill the bowl with argon, after safety closure device was closed, air in the bowl was evacuated by a vacuum pump through the gas outlet of the lid of the bowl. Then, the bowl was back filled with

argon from the gas inlet for 10 minutes with a flow rate of 250cc/min. Experimental parameters used in ball milling for mechanochemical synthesis are given in Table 3.3.

Table 3.3 Experimental Parameters used in Ball Milling for MCP

Ball Milling for MCP	Medium	Sequence	Atmosphere	Sizes and quantities of balls	Ball Milling Rate (rpm)	Ball Milling Duration (hour)
	Dry Ball Milling	-	Argon	12 pieces with 20 mm diameter	300	15
		Before Ignition	Argon	6 pieces with 20mm diameter	300	5

3.6 Leaching Process

Leaching is the process of bringing a solid in contact with an aqueous solvent with the objective of dissolving one or more of the compounds contained in the solid [77]. This process results in more concentrated desired part of the material [78].

Dissolution rate of the part wanted to be dissolved in the solid material is affected by many factors such as the leaching agent (solvent), its concentration, temperature of the leaching solution, and duration of leaching. Leaching agent should be chosen such that the part of the powder wanted to be removed from the solid should be soluble in the leaching solvent while the part which is desired to remain in the solid should be insoluble or less soluble in it [78].

The reaction products consisting of TiB_2, MgO and minor components like $Mg_3B_2O_6$, Mg_2TiO_4, MgB_2 and TiN were leached with HCl with the objective of dissolving all components other than TiB_2 so as to obtain pure TiB_2.

After products were leached, molar yield of produced TiB_2 was calculated according to equation given below:

$$\text{Molar Yield} = \frac{\text{Weight of Leached Sample}}{\text{Weight of Unleached Sample} \times 0.2564} \times 100 \qquad (3.3)$$

where 0.2564 is the weight fraction of TiB_2 in the unleached sample calculated in accord with the stoichiometry of Reaction (3.1).

For leaching of the products 1, 3, 5, 7 M HCl solutions were prepared. Concentration of these solutions was adjusted as follows:

According to the data supplied by the manufacturer, HCl solution contains 37 wt% HCl in water. First, molarity of used HCl (37 wt%) was calculated. (Molecular Weight of HCl = 36.46 g/mol)

$$\text{Molarity of used HCl} = \frac{37g \text{ HCl}}{100g \text{ soln.}} \times \frac{1mol}{36.46 \text{ g}} \times 1.19 \frac{g \text{ soln}}{mL \text{ soln.}} \times 1000 \frac{mL}{L} = 12.076 \frac{mol}{L}$$

According to this calculation in order to prepare 1M, 1L HCl solution, $\frac{1}{12.076 \text{ mol/L}} = 0.083\,L = 83mL$ HCl (37wt%) was taken and mixed with 917 mL deionized water.

3.6.1 Leaching Process without Heating

The experimental set-up used in leaching (stirring) without heating is shown in Fig.3.9. In the leaching process, firstly, magnetic stirring bar was put into a glass beaker. Then, HCl of a given concentration was added and the beaker was put onto the plate of the magnetic stirrer. After that, watch glass was placed on the beaker in

order to prevent splash of the mixture during stirring process. Finally, the stirrer was operated for a predetermined period.
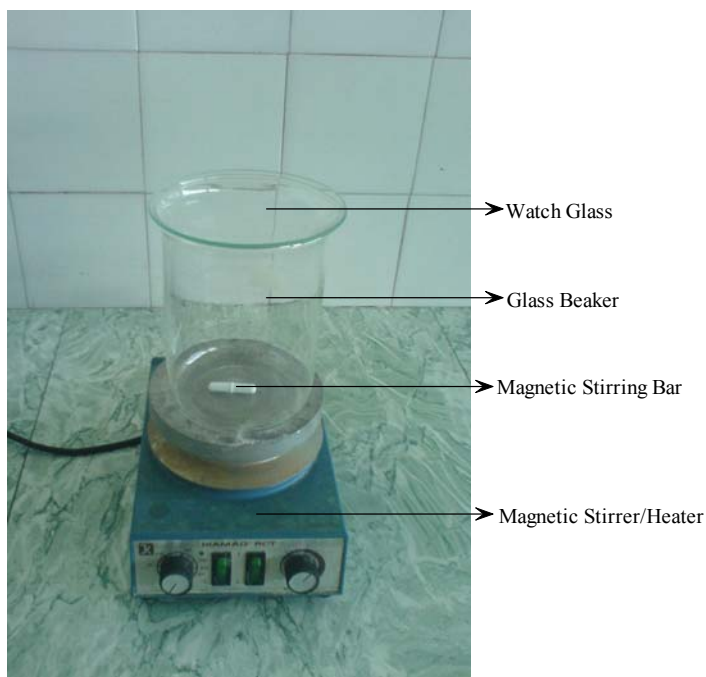
Fig.3.9 Experimental set-up of leaching without heating

After leaching, filtration of the sample was made. During this process, the following steps were used: Firstly, pump was operated and filter paper, which was placed into the Buechner funnel, was wetted with deionized water. Then, sample-solution mixture in the beaker was poured onto the filter very slowly in order to prevent splashing of the sample on the side of the Buechner funnel. Due to the operating vacuum pump, aqueous part was collected in the flask easily and wet solid, which was the product of the leaching, remained on the filter paper (Fig.3.10). After filtration, the solid sample remaining on the filter paper was washed with deionized water. After washing, solid with filter paper was taken out of the Buechner funnel and was put onto a watch glass. Then, watch glass was placed into the drying oven

preheated to 90 °C and kept there for about 20 minutes. Filtrate in the flask was filtered again by repeating above procedures using a second filter paper in order to take remaining part of the solid sample in the liquid because during first filtration, some solids entered the filtrate. After drying the solid was removed from the surface of the filter paper by scraping.
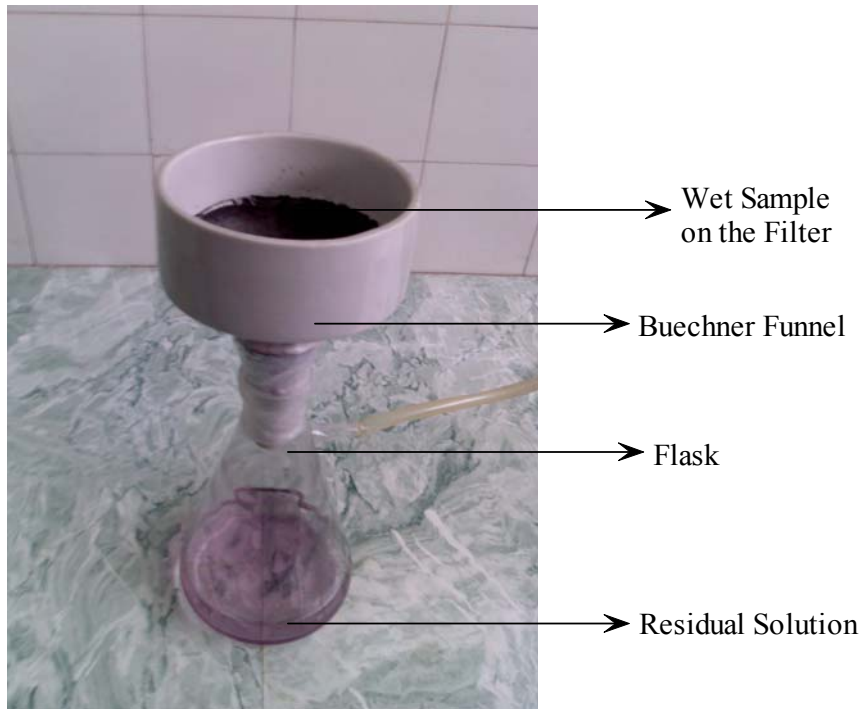
Fig.3.10 Experimental set-up of filtration and obtained sample and residual solution

3.6.2 Leaching Process with Heating

Schematic drawing of the set-up, which was used in the leaching process with heating, is given in Fig.3.11. In this process, a Velp Scientifica AREX2 hot plate/ magnetic stirrer, a 250 ml Pyrex balloon with three necks, a contact thermometer

having ± 2°C sensitivity, a water cooled Liebig condenser column and a magnetic stirring bar were used.

Firstly magnetic stirring bar (magnet) was put into the balloon and it was placed onto the magnetic stirrer/heater. Then, a condenser column was attached to the system in order to avoid vaporization losses. In order to keep temperature constant a thermometer was inserted into the balloon. Finally, powder and solution was fed to the system as shown in Fig.3.11. Then, the lid of the neck of the balloon was closed and heater/stirrer was operated. In this study, leaching with heating experiments were conducted in solutions at 75 $^{\circ}$C.

Fig.3.11 Experimental set-up of leaching with heating

After leaching, filtration process was done similar to filtration process in leaching without heating.

3.7 X-Ray Diffraction and Microscopic Studies

After all these processes, in order to examine the formed phases; ignition products, ball milled products and leached products were analyzed by a Rigaku Multiflex Powder X-Ray diffractometer (XRD) with Cu-Kα radiation at the Department of Metallurgical and Materials Engineering of METU in the 2θ range of 20° to 80° with 0.02^o steps at a rate of 2°/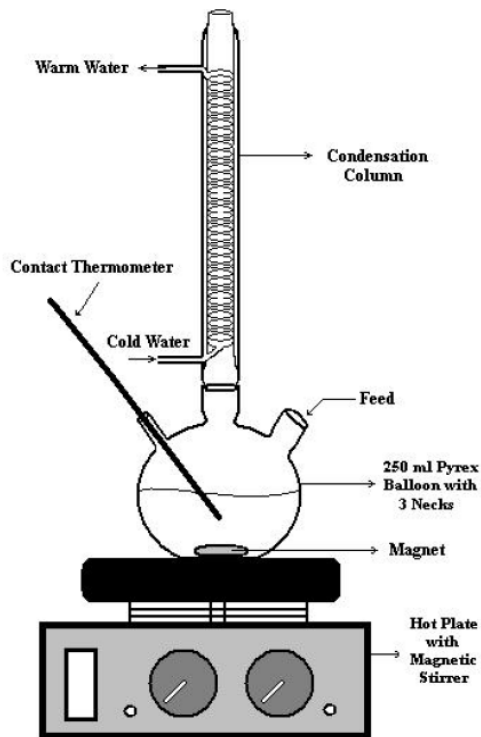min. Smoothing, background subtraction, Kα2 elimination and phase identification operations were performed on the XRD patterns by the Qualitative Analysis Program. In addition, in order to examine particle size and morphology of the products a Jeol JSM 6400 scanning electron microscope (SEM) at the Department of Metallurgical and Materials Engineering of METU was used.

Using XRD pattern of samples, average crystal size of the products was calculated using Scherrer formula [79, 80].

$$L_c = \frac{0.9 \times \lambda}{B \times \cos\theta_B} \tag{3.4}$$

where L_c is the average crystal size, λ is the wavelength (1.54056 A^o, for CuKα), θ_B is the Bragg angle. B is the line broadening, in radians, by reference to a standard, so that

$$B^2 = B_M^2 - B_S^2 \tag{3.5}$$

where B_S is the width of the standard material in radians and B_M is the measured value of the full width at half maximum of the peak on the XRD pattern. In the measurements a peak of a silicon standard at 2θ of 28.41^o was used to determine B_S, which had a width of 0.15^o.

CHAPTER IV

RESULTS AND DISCUSSION

4.1 Determination of Reaction Temperature

Since there was no information in the literature about the temperature at which titanium diboride is produced with Reaction (4.1), initial experiments were performed in order to determine the ignition temperature of this reaction.

$$TiO_2 + 2H_3BO_3 + 5Mg = TiB_2 + 5MgO + 3H_2O \qquad (4.1)$$

Reactant mixture was prepared according to the stoichiometry of Reaction (4.1) and placed into the pot furnace which was preheated to selected temperatures according to the procedure given in Chapter III. A puffing sound which indicated the occurrence of the reaction was heard in 5 minutes. After that, the crucible was taken out from the furnace. Since obtained products were fragile and in the form of a sponge, they could be ground in the mortar. This experiment was repeated for furnace preheat temperatures of 600, 700, 725, 750, and 800 ^{o}C. In order to determine which phases existed in the reaction products, powder X-Ray Diffraction (XRD) method was used. XRD patterns obtained from these experiments are presented in Fig.4.1.
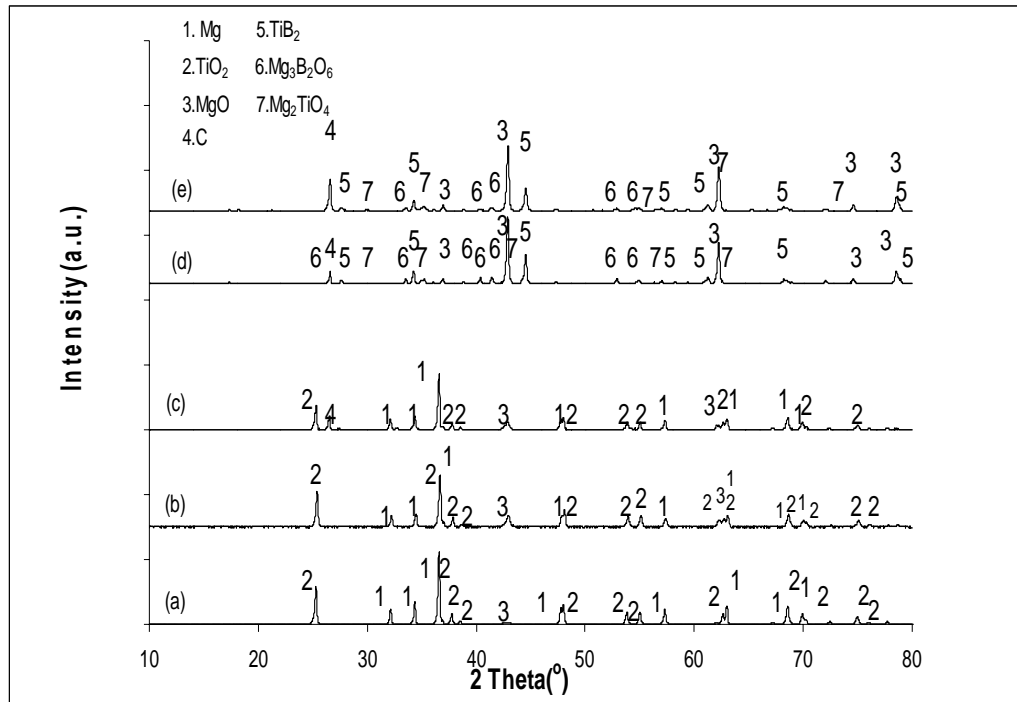
Fig.4.1 Effect of temperature on TiB$_2$ production from H$_3$BO$_3$ + Mg + TiO$_2$ mixtures (a) 600 ^{o}C, (b) 700 ^{o}C, (c) 725 ^{o}C, (d) 750 ^{o}C, (e) 800 ^{o}C

It is seen that at temperatures of 600, 700, and 725 ^{o}C the reaction did not take place. In addition, oxidation of Mg was observed at temperatures higher than 600 ^{o}C. Product phases were observed in the samples placed to the furnace heated to 750 ^{o}C and 800 ^{o}C. These results indicated that Reaction (4.1) started at a temperature between 725 ^{o}C and 750 ^{o}C. In order to determine the temperature at which the reaction starts more accurately, ignition temperature determination experiments whose procedure was given in Chapter III were conducted. In these experiments, a hole was drilled on the lid of the crucible and a K type thermocouple was inserted into it. The thermocouple was in touch with the reactants. Temperatures recorded in the experiment conducted in the furnace preheated to 800 ^{o}C are presented in Fig.4.2. A steep temperature rise is observed from this Figure at 745 ^{o}C; puffing was heard at about this temperature during the experiment. Therefore, the ignition temperature may be considered to be 745 ^{o}C at which temperature increases abruptly due to the

reaction being exothermic. Since the ignition temperatures are expected to depend on the heating rate of the reactants, it was kept constant at approximately 160 ^{o}C/minute in the ignition temperature experiments. An ignition temperature determination experiment was made in which the reactant mix consisted of TiO_2, Mg and B_2O_3 instead of H_3BO_3. Temperature-time curve recorded in this experiment is also given in Fig.4.2 from which the abrupt temperature rise is seen at 693 ^{o}C. This result indicates that it is possible to reduce ignition temperature to 693 ^{o}C with igniting B_2O_3 containing starting mixture prepared according to Reaction (4.2). B_2O_3 used in this experiment was produced by calcination of H_3BO_3 in the furnace at 900 ^{o}C for 45 minutes.

$$TiO_2 + B_2O_3 + 5Mg = TiB_2 + 5MgO \qquad (4.2)$$

The reason of the decrease in ignition temperature may be calcination of H_3BO_3 by the following reaction:

$$H_3BO_3 = 1/2\ B_2O_3 + 3/2\ H_2O \qquad (4.3)$$

When H_3BO_3 was used, heat was consumed for calcination of H_3BO_3 and this may cause the reaction to take place at higher temperatures.
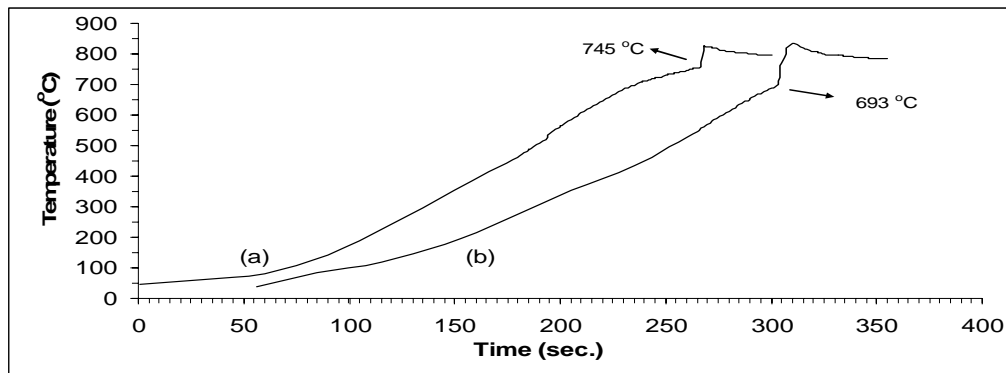

Fig.4.2 Effect of using (a) H_3BO_3, (b) B_2O_3 on ignition temperature (plot (b) was shifted 55 seconds to right for clarity)

Puffing did not take place in the experiment conducted with B_2O_3. As a result, puffing sound heard while using H_3BO_3 may be due to release of chemically bonded water in the H_3BO_3 powder. Since the reactant mixture was placed into the furnace at 800 ^{o}C, ignition occurring before complete calcination of H_3BO_3 (Reaction (4.3)) may have caused the puffing of powders with a sound. In addition, during the sudden increase in the temperature when ignition takes place as shown in Fig.4.2, air and formed water steam in the crucible may have expanded and caused the puffing.

4.2 Effect of Excess Mg

XRD patterns of the reaction products obtained from experiments conducted at 750 and 800 ^{o}C, shown in Fig.4.1(d) and Fig.4.1(e), respectively, indicate that two minor phases, Mg_2TiO_4 (magnesium titanate) and $Mg_3B_2O_6$ (magnesium borate), are present in the reaction products in addition to the expected TiB_2 and MgO phases.

Use of excess magnesium may have an effect on formation of the minor phases Mg_2TiO_4 and $Mg_3B_2O_6$. With this consideration, experiments were conducted by use of excess magnesium.

Firstly, 10% excess Mg was added into reactant mixture and it was put into the crucible and the crucible with its contents was placed into the furnace preheated to 800°C. After ignition, the crucible was taken out of the furnace. Then, the same procedure was repeated for 20%, 30%, and 40% excess Mg. XRD patterns of the obtained products are given in Fig.4.3.
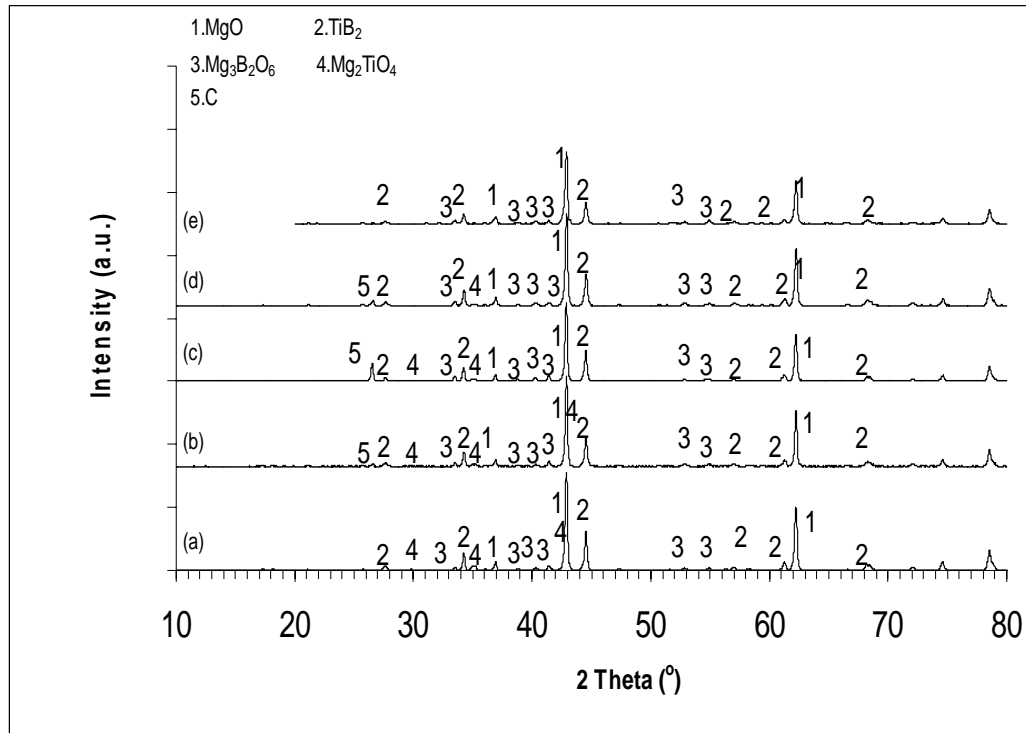
Fig.4.3 Effect of excess Mg addition on minor phases (a) Stoichiometric amount Mg, (b) 10% excess Mg, (c) 20% excess Mg, (d) 30% excess Mg, (e) 40% excess Mg

Relative peak intensity of the Mg_2TiO_4 phase is seen to decrease with increase in the amount of excess Mg from Fig.4.3; no Mg_2TiO_4 phase is observed to be present in the reaction product of the experiment conducted by use of 40% excess Mg. Amount of the excess Mg used appear to have no effect on the amount of $Mg_3B_2O_6$ from Fig.4.3. It was concluded from these results that formation of Mg_2TiO_4 could be prevented by use of 40% excess Mg but use of excess magnesium did not have an effect on formation of $Mg_3B_2O_6$.

4.3 Leaching Studies

In order to remove mainly MgO and also minor phases, leaching experiments whose procedure was given in Chapter III were conducted. In this process, leaching was

performed for 15 hours in the HCl / water solution whose concentration was predetermined. Slurry density was 1/100 (g/cc) and leaching was performed at room temperature. After leaching, the solution was filtered using S&S brand filter papers with blue band, which are used for filtering of fine particles.
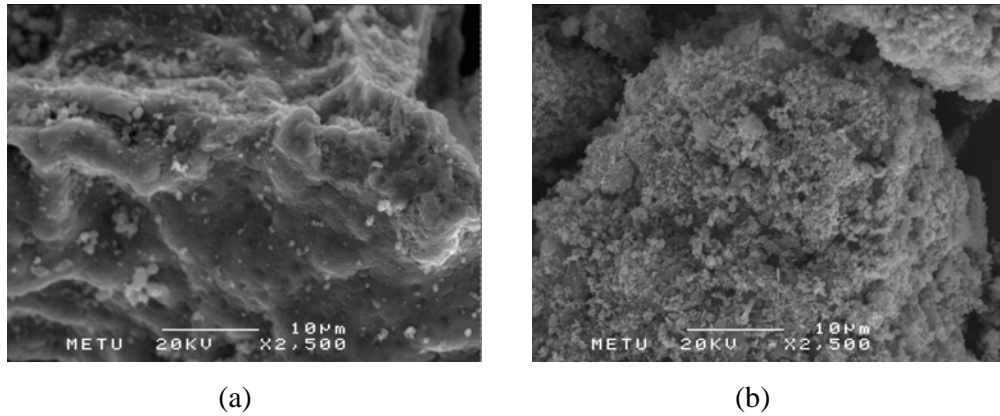

(a)   (b)

Fig.4.4 SEM micrographs of (a) Ignited sample in the furnace preheated to 800 ^{o}C, (b) Sample leached for 15 hours in the 1M HCl solution after ignition

SEM micrographs of the sample produced by ignition in the furnace preheated to 800 ^{o}C before and after leaching are given in Fig.4.4(a) and Fig. 4.4(b), respectively. Leaching is observed from Fig.4.4(b) to result in a sponge like structure. It may, therefore, be inferred that the structure in Fig.4.4(a) is converted to the porous structure of Fig.4.4(b) due to Mg_2TiO_4, $Mg_3B_2O_6$ and mainly MgO being leached.

XRD patterns of the sample produced by ignition in the furnace preheated to 800 ^{o}C before and after leaching are given in Fig.4.5(a) and Fig.4.5(b). It can be seen that peaks of MgO were almost completely removed in the leaching process. In addition, a peak of MgB_2 was observed in the XRD patterns of the leached sample. Since after leaching MgO peak was lowered, MgB_2 peak which was placed at the same position with the MgO became more distinguishable. Furthermore, a peak of TiN appeared because experiments were conducted in air atmosphere. Moreover, minor phases

were still observed in the XRD patterns given in Fig.4.5. This may result from insolubility of the minor phases in the 1 M HCl solution.
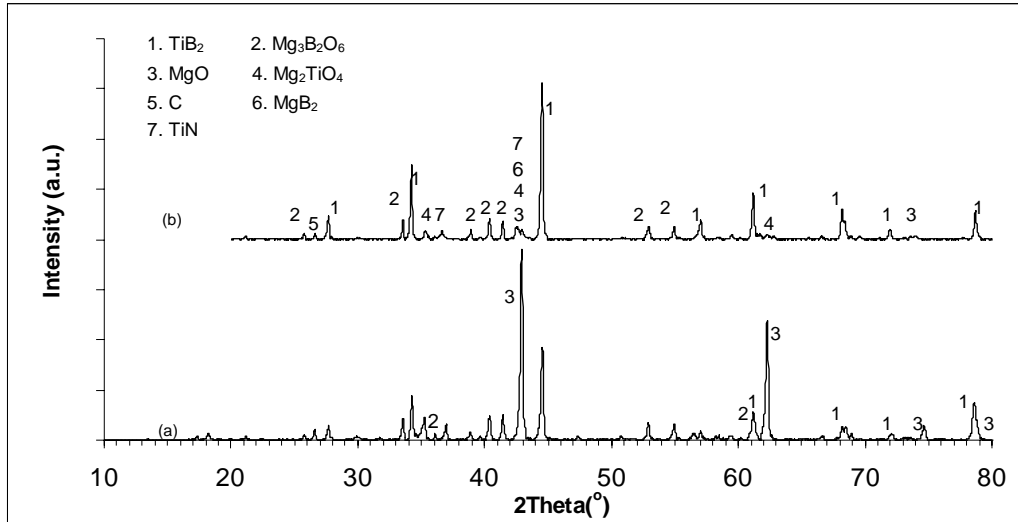
Fig.4.5 XRD pattern of (a) Sample ignited in furnace preheated to 800 $^{\circ}$C, (b) Sample in (a) leached in the 1M HCl solution for 15 hours

It was thought that solubility of the minor phases can be increased by decreasing the particle size. Since ball milling would provide a decrease in particle size of the powder and ball milled powders may become more soluble in the 1M HCl solution, reaction products were decided to be ball milled before leaching. The particle size of TiB_2 powder was not expected to decrease when using ball milling since TiB_2 is very hard.

Ball milling was conducted for 7 hours with 150 revolutions per minute (rpm). The ball was set to stop every hour and then start in the reverse direction after 5 minutes of waiting. In the ball milling experiment, 50 stainless steel balls having 10 mm diameter were used.

SEM micrographs of the reaction product obtained from the reaction mix ignited in the furnace preheated to 800 $^{\circ}$C before and after ball milling shown in Fig.4.6(a) and Fig.4.6(b), respectively, indicate that agglomerates are broken by ball milling.

(a)	(b)
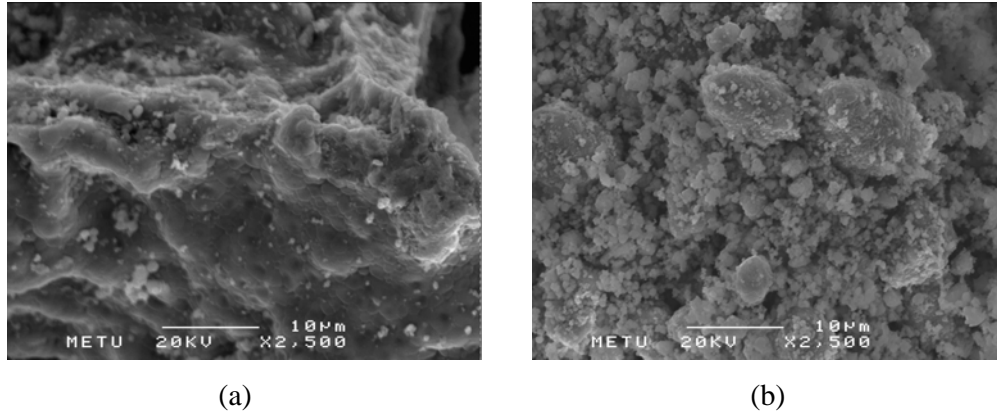
Fig.4.6 SEM micrographs of (a) Sample ignited in the furnace preheated to 800 $^{\circ}$C, (b) Sample dry ball milled for 7 h with 150 rpm after ignition in the same conditions

XRD patterns of the ignition product directly leached and leached after ball milling are presented in Fig.4.7(a) and Fig.4.7(b), respectively.

Fig.4.7 indicates that there is no difference in the XRD patterns of the two samples. It can therefore be stated that dry ball milling does not have any beneficial effect on the removal of the minor phases from the ignition product. In other words, dry ball milling after ignition did not change the leaching behavior of the ignition products effectively.
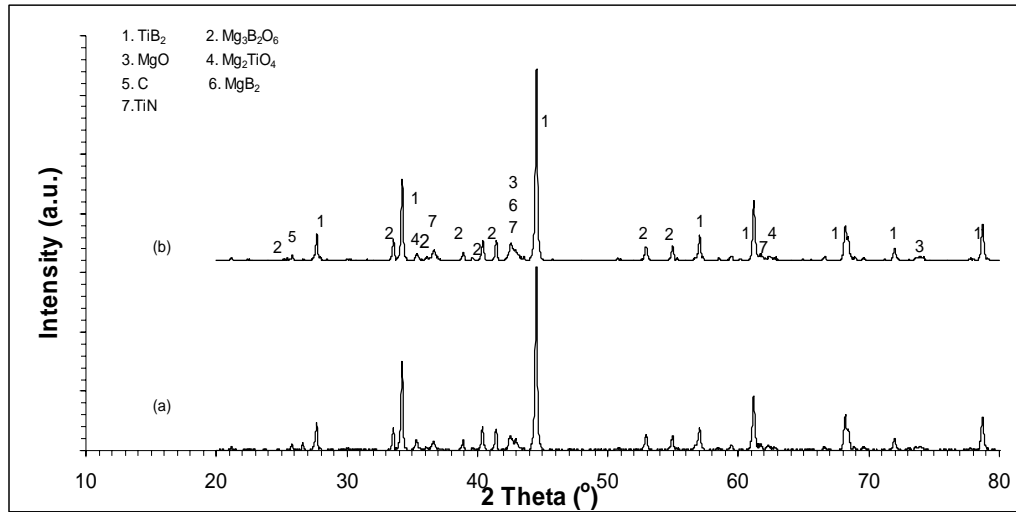
Fig.4.7 Effect of ball milling process performed after ignition (a) Sample ignited, leached for 15 h in 1M HCl, (b) Sample ignited, ball milled for 7 h and leached for 15 h in 1M HCl

In order to obtain finer particles, which would help to increase the rate of dissolution [73] of the undesired phases in the leaching solution, ball milling was decided to be made in the liquid medium. In the experiments, ethanol (C_2H_5OH) which does not react with TiB_2 [27] was decided to be used as the liquid medium. In the ball milling process, approximately 40 ml ethanol and 50 pieces of 10 mm diameter balls were used. Milling was performed for 7 hours with 150 rpm. XRD patterns of the ignition product leached after dry ball milling and after wet ball milling are given in Fig.4.8(a) and Fig.4.8(b), respectively.
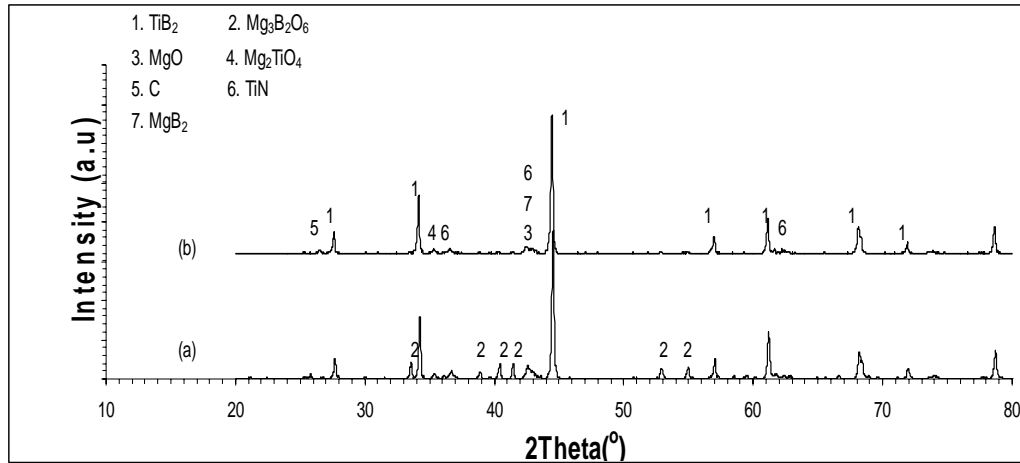
Fig.4.8 Effect of ball milling with ethanol medium after ignition (a) XRD of sample ignited, ball milled and leached in the 1M HCl, (b) Sample ball milled in ethanol, leached in the same condition with other sample after ignition again with the same conditions

As it is seen from Fig.4.8 (b), peak of $Mg_3B_2O_6$ was not observed while Mg_2TiO_4 was observed after leaching following wet ball milling. Therefore, it is possible to say that ball milling in the ethanol medium after ignition in the furnace results in elimination of the magnesium borate minor phase after leaching in 1M HCl solution; ball milling in ethanol does not have an effect on leaching of Mg_2TiO_4.

SEM micrographs of the ignition product directly leached and leached after wet ball milling are given in Fig.4.9(a) and Fig.4.9(b), respectively.

Fig.4.9 (b) shows that ball milling in the ethanol medium before leaching helps breaking up the agglomerates. This may be taken as an indication that ball milling in the ethanol medium liberates the particles and reduces the particle size.
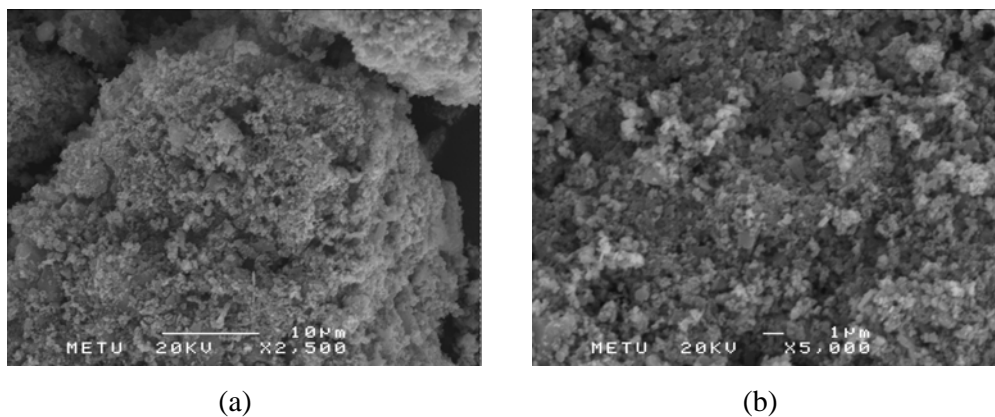
(a)   (b)

Fig.4.9 SEM micrographs of (a) Sample leached for 15 h in 1 M HCl after furnace ignition, (b) Sample furnace ignited, ball milled for 7 h with 150 rpm in ethanol and leached for 15 h in 1 M HCl

The reason of elimination of $Mg_3B_2O_6$ at the end of wet ball milling and HCl leaching may be due to size reduction as a result of the ball milling process or it may be due to dissolution of $Mg_3B_2O_6$ in ethanol. In order to understand which reason given in the previous statement was effective, the ignited sample was stirred in ethanol in a glass beaker by a magnetic stirrer for 7 hours, filtered and leached in the 1M HCl for 15 hours. XRD pattern of the product of this process is given in Fig.4.10(b); XRD pattern of the ignited sample leached in HCl after ball milling in ethanol is given in Fig.4.10(a).

Peaks related to $Mg_3B_2O_6$ are observed in Fig.4.10(b) indicating that $Mg_3B_2O_6$ does not dissolve in ethanol. Based on the result it is possible to say that elimination of $Mg_3B_2O_6$ results from the size reduction due to ball milling in the ethanol medium which helps to grind the particles more efficiently, and increase the rate of dissolution of $Mg_3B_2O_6$ in the HCl solution.
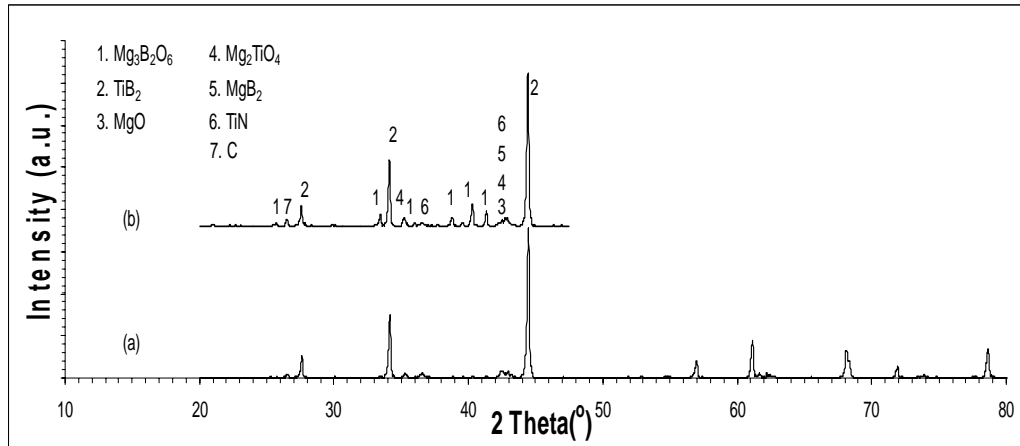
Fig.4.10 (a) Sample ignited, ball milled in ethanol and leached in the 1M HCl for 15 h, (b) Sample ignited, stirred in ethanol, filtered, leached 1 M HCl for 15 h

As stated above, use of 40% excess Mg in the reaction mix results in Mg_2TiO_4 not to form during ignition and $Mg_3B_2O_6$ forming during ignition can be eliminated by leaching of the sample ball milled in ethanol. In order to eliminate both of the minor phases, sample containing 40% excess Mg was ignited in the furnace, ball milled in ethanol and leached in 1 M HCl solution.

XRD patterns of the leach products of the samples obtained from reaction mixes containing stoichiometric amount of Mg and 40% excess Mg are given in Fig.4.11(a) and Fig.4.11(b), respectively. As can be seen from Fig.4.11(b), Mg_2TiO_4 peaks were not observed in the sample containing 40% excess Mg. In addition, no peak related to $Mg_3B_2O_6$ was observed owing to ball milling in the ethanol. However, the intensity of the peak resulting from TiN and MgB_2 increased probably due to addition of excess Mg. TiN formation may have taken place through reduction and nitridation of TiO_2 according to Reaction (4.4). Due to this reaction when excess Mg was used, relative peak height of TiN increased. The source of N_2 is the air inside the graphite crucible.

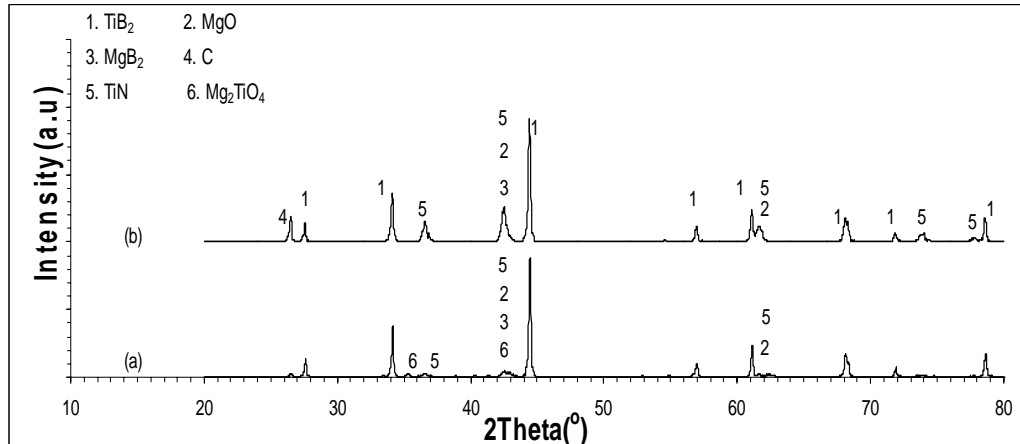$$2TiO_2 + 2Mg + N_2 = 2TiN + 2MgO \tag{4.4}$$

Fig.4.11 Effect of 40% excess Mg on the XRD patterns of leached samples. (a) Sample containing stoichiometric amount Mg after ignition, ball milling for 7 h in ethanol and leaching for 15 h in 1 M HCl, (b) Sample containing 40% excess Mg after ignition, ball milling and leaching with the same conditions

All leaching operations in the experiments reported above were conducted with 1 M HCl by the use of which MgB_2, TiN and the all of the MgO could not be eliminated from the reaction products. Based on this result, concentration of HCl was decided to be increased and leaching was conducted in 3 M HCl. XRD patterns of the products leached in 1 M HCl and 3 M HCl are given in Fig4.12(a) and 4.12(b), respectively; both of these samples were products obtained from stoichiometric mixes ignited in the furnace preheated to 800 ^{o}C and ball milled in ethanol. Leaching in 3 M HCl is seen to eliminate Mg_2TiO_4, $Mg_3B_2O_6$ and MgO but not to affect the peaks of MgB_2 and TiN. This result shows that it is possible to obtain a product not containing Mg_2TiO_4 by leaching in 3 M HCl and that use of 40% excess Mg is not necessary to obtain a Mg_2TiO_4 – free product.
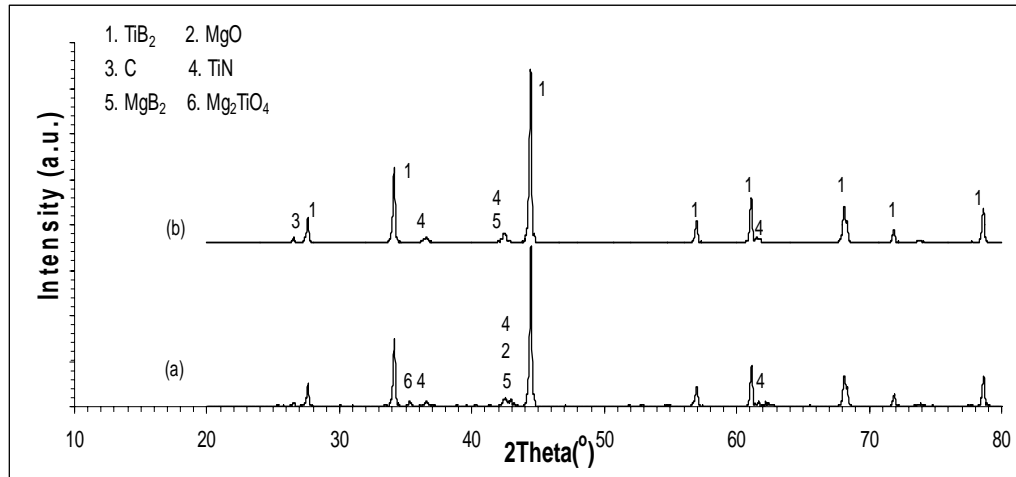
Fig.4.12 Effect of concentration of HCl on the leached products (a) Sample ignited, ball milled for 7 h in ethanol and leached for 15 h in 1 M HCl, (b) Sample ignited, ball milled for 7 h in ethanol and leached for 15 h in 3 M HCl

With the procedures used up to now, MgB_2 and TiN could not be eliminated. The quantities of both of these phases were found to increase by use of excess magnesium as stated above. To find whether use of less than the stoichiometric amount of Mg would have an effect on the quantities of MgB_2 and TiN forming, an experiment was made with a reaction mix containing 10% excess TiO_2 and 20% excess B_2O_3. This mix was ignited in the furnace preheated to 800 ^{o}C, ball milled for 7 hours in ethanol and then leached in 3 M HCl. XRD patterns of the leached products obtained from the stoichiometric mix and the Mg-deficient mix are given in Fig.4.13(a) and 4.13(b), respectively. Use of less than the stoichiometric amount of Mg is seen not to affect the quantities of MgB_2 and TiN and to result in the presence of Mg_2TiO_4 in the leached product. Based on this result, use of non-stoichiometric mixes was considered not to be beneficial and all of the subsequent experiments were conducted with stoichiometric mixes.
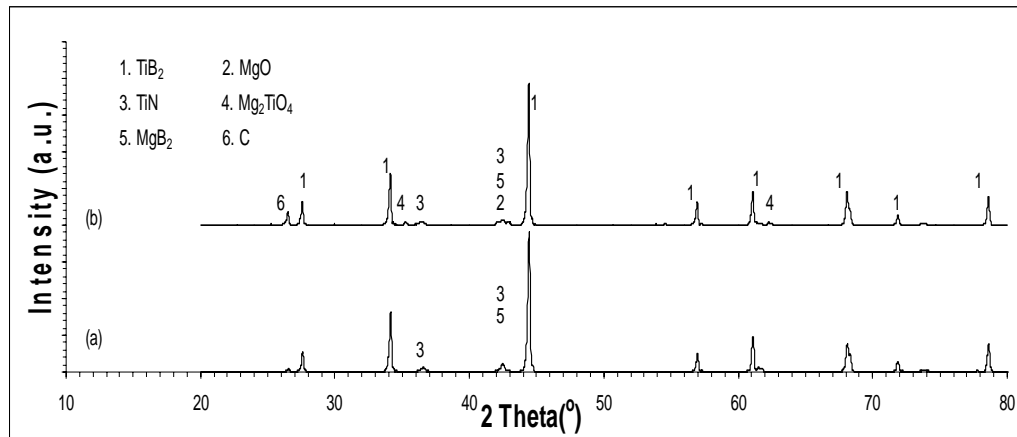
Fig.4.13 XRD pattern of (a) Sample ignited, ball milled for 7 h in ethanol and leached for 15 h in 3 M HCl, (b) Sample containing 10 % excess TiO_2 and 20 % excess B_2O_3 after ignition, ball milling for 7 h in ethanol and leached for 15 h in 3 M HCl

It was not possible to eliminate MgB_2 and TiN from the reaction products by leaching in 1 M HCl and 3 M HCl solutions. In the next set of experiments products obtained by ignition of stoichiometric mixes in the furnace preheated to 800 ^{o}C were leached in 5 M HCl and 7 M HCl solutions after ball milling in ethanol. XRD patterns of the samples leached in 5 M HCl and 7 M HCl solutions are presented in Fig.4.14(c) and Fig.4.14(d), respectively, together with the XRD patterns of the samples leached in 1 M HCl and 3 M HCl solution given in Fig.4.14(a) and Fig.4.14(b), respectively. As can be seen from this figure, $Mg_3B_2O_6$ and most of MgO can be eliminated from the product by leaching in 1 M HCl. Leaching in 3 M HCl result in elimination of Mg_2TiO_4 from the system also. Leaching in 5 M HCl is seen to additionally eliminate MgB_2 from the system. TiN is seen not to be eliminated from the product even leaching in 7 M HCl.
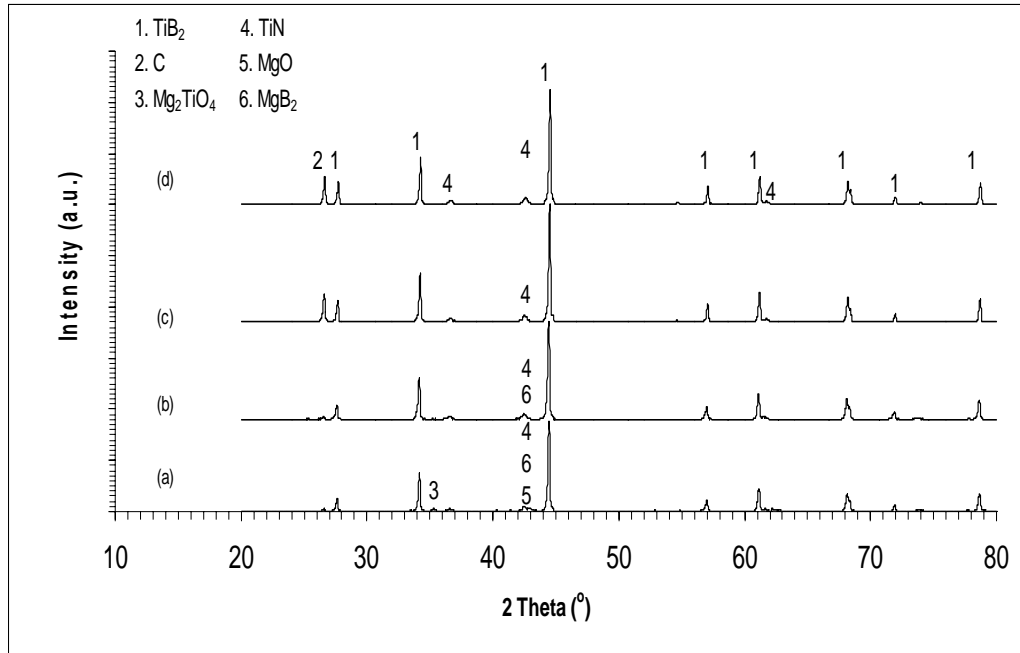
Fig.4.14 XRD pattern of sample ignited, ball milled for 7 h in ethanol, leached for 15 h in (a) 1 M HCl, (b) 3 M HCl, (c) 5 M HCl and (d) 7 M HCl

TiN was stated above to form by a reaction involving $N_2(g)$ originating from air. In order to prevent formation of TiN, ignition was decided to be conducted under argon atmosphere. A stoichiometric mix was ignited under Ar atmosphere in the furnace preheated to 800 ^{o}C the product of which was leached in 5 M HCl solution after ethanol ball milling. XRD pattern of the leached product obtained in this experiment is given in Fig.4.15. This product is seen to be pure TiB_2.

Fig.4.15 XRD pattern of sample ignited under argon atmosphere, ball milled in the ethanol medium and leached in 5 M HCl solution

Based on the results presented above, it can be stated that pure TiB_2 can be produced by the following procedure: (1) Ignition of a stoi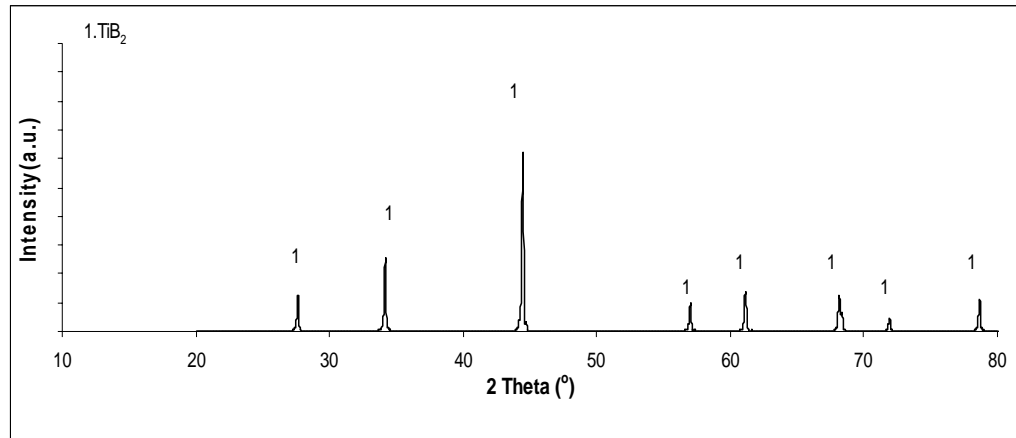chiometric TiO_2 + B_2O_3 + Mg mix under argon atmosphere, (2) Ethanol ball milling of the product of the ignition, and (3) Leaching of the ethanol ball milled sample in 5 M HCl. The weight of the TiB_2 obtained at the end of this procedure was 30% of the weight to be obtained stoichiometrically based on Reaction (4.2). This low yield of TiB_2 is due to the fact that phases like $Mg_3B_2O_6$, Mg_2TiO_4 form during ignition and that some TiB_2 is lost during leaching due to dissolution of TiB_2 in HCl.

In the production of pure TiB_2 ball milling process was used. However, it is a time consuming and tedious process. In order to produce pure TiB_2 without ball milling, leaching experiment was conducted with heating. Heating during leaching process is expected to increase the efficiency of leaching. In order to perform leaching with heating, a stoichiometric mix was ignited under argon atmosphere and the product of ignition was leached in 5 M HCl solution at 75 $^{\circ}$C for 15 hours. XRD pattern of the solid obtained at the end of leaching in this experiment is given in Fig.4.16.
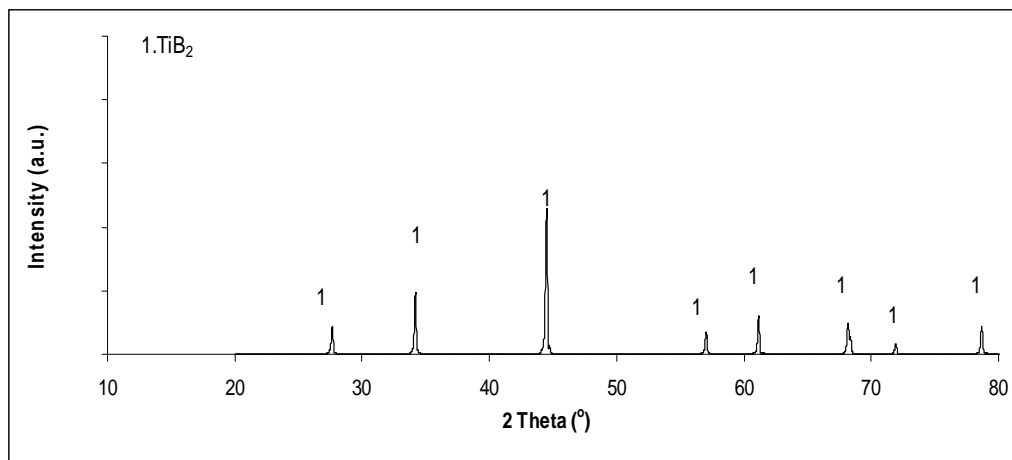
Fig.4.16 XRD pattern of sample ignited in argon and leached in 5 M HCl for 15 hours at 75 $^{\circ}$C

As can be seen from Fig.4.16, the product of this experiment contained no minor phases and it was pure TiB_2. The yield of TiB_2, i.e., the weight of TiB_2 obtained as a percentage of the weight of TiB_2 to be obtained stoichiometrically based on Reaction (4.2), was 48.6%.

Based on the results presented above, it can be stated that pure TiB_2 can be produced by the following procedure: (1) Ignition of a stoichiometric TiO_2 + B_2O_3 + Mg mix under argon atmosphere and (2) Leaching of the ignited sample in 5 M HCl solution at 75 $^{\circ}$C.

4.5 Mechanochemical Synthesis

Ball milling for mechanochemical synthesis was firstly applied to the stoichiometric mix under Ar for 5 hours at 300 rpm with 6 pieces of balls having 20 mm diameter. XRD pattern of 5 hour ball milled sample is given in Fig.4.17(a). It was seen from this figure that at the end of 5 hours of ball milling, peaks of TiO_2 and Mg were present. Due to the amorphous structure of B_2O_3 which results from rapid cooling of

liquid boric oxide, its peaks did not present in the XRD pattern. The presence of reactants and absence of expected products in the XRD analyses indicate that no reaction took place in 5 hours of ball milling.
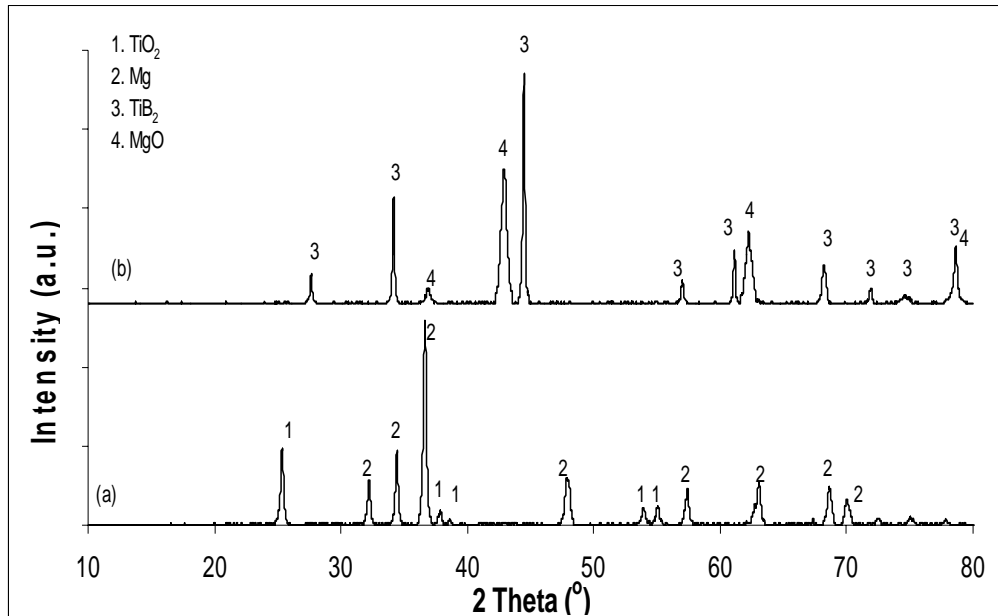
Fig.4.17 XRD pattern of (a) Sample ball milled for 5 hours, (b) Sample ball milled for 15 hours

Since after 5 hour ball milling, reaction did not take place, ball milling was decided to be performed for 15 hours at 300 rpm under argon atmosphere with 12 pieces of balls having 20 mm diameter. XRD pattern of sample ball milled for 15 hours is given in Fig.4.17(b). As can be seen from this figure, there are peaks of only TiB_2 and MgO, indicating that the reaction was complete. No unreacted species were detected in the XRD pattern of the products. All of the reactants may have been consumed or it is possible that some of the reactants were ground so fine that they had amorphous structure.

TiB$_2$-MgO product, obtained at the end of 15 hours of ball milling, was leached in HCl solution in order to remove MgO. It is known that TiB$_2$ is slightly soluble in HCl solutions and some TiB$_2$ may be lost during leaching. Therefore, before leaching, in order to determine the minimum possible leaching duration and acid concentration, leaching behavior of pure MgO in dilute HCl has been investigated. It was seen that MgO did not dissolve completely in 0.25 M HCl solution at a solid to leachant ratio of 1/100 (g/cc). However, pure MgO was found to dissolve completely in 0.5 M HCl solution in 3 minutes. Consequently, TiB$_2$-MgO product was leached in 0.5 M HCl solution for 3 minutes. It can be seen in Fig.4.18 that MgO was completely removed and pure TiB$_2$ phase was obtained. Molar yield of TiB$_2$ obtained by ball milling for 15 hours and leaching for 3 minutes in 0.5 M HCl solution was calculated as 89.6%. This value was 86.1% after 15 minutes of leaching and it was 76.6% after 2 hours of leaching in 1 M HCl solution. These results indicate that there is some loss of TiB$_2$ due to its dissolution in HCl solution.
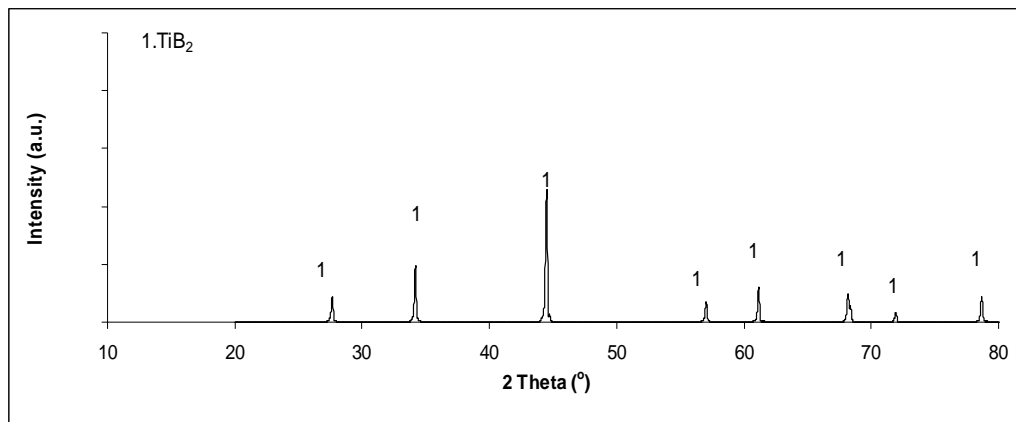

Fig.4.18 XRD pattern of sample ball milled for 15 hours and leached for 3 minutes in 0.5 M HCl solution

As shown in Table 4.1, molar yield of TiB$_2$ produced by mechanochemical synthesis was much higher than that of the yield obtained from volume combustion

experiments (30%). After mechanochemical synthesis of TiB_2, in order to remove MgO from the products, lower concentration of HCl and shorter leaching duration was sufficient. This, together with the fact that no minor phases like Mg_2TiO_4, $Mg_3B_2O_6$ etc. form results in the molar yield of TiB_2 produced by mechanochemical method being higher. The possibility of shorter duration of leaching of the mechanochemically obtained products may be attributed to the smaller particle size of the formed MgO and also the absence of side products such as Mg_2TiO_4 or TiN. The average crystal size of formed MgO in the mechanochemical synthesis after 15 h ball milling was 17.22 nm, as calculated by the Scherrer formula. On the other hand, average crystal size of MgO formed after volume combustion synthesis was calculated as 47.18 nm. These results indicate that MgO obtained after mechanochemical synthesis had much smaller crystallites, which provides an easier leaching.

Table 4.1 Molar yield of TiB_2 obtained in different processes

	Molarity of HCl	Leaching Duration	Molar Yield (%)
Ball mill +	1	2 hours	76.6
Leaching	1	15 minutes	86.1
	0.5	3 minutes	89.6
Ignition (air)+	1	15 hours	57.0
Ethanol Ball Mill	3	15 hours	44.6
+ Leaching	5	15 hours	33.0
Ignition (argon)+ Ethanol Ball Mill+ Leaching	5	15 hours	30.0
Ignition(argon) + Leaching at 75°C	5	15 hours	48.6

SEM micrograph of TiB_2 produced by mechanochemical processing is presented in Fig.4.19. According to the measurements performed on SEM micrographs, produced TiB_2 had an average particle size of 0.27±0.08 µm. This value was obtained by measuring the size of at least 50 particles, and calculating their average and standard deviation. TiB_2 powder obtained by ignition (volume combustion) did not present a noticeable difference in particle size, as observed from SEM micrograph.

Average crystal size of TiB_2 formed in volume combustion synthesis and mechanochemical processing was not much different. It was 32.18 nm when produced mechanochemically and it was 40.65 nm after volume combustion. Higher crystal size was an expected result in volume combustion due to higher temperature attained.
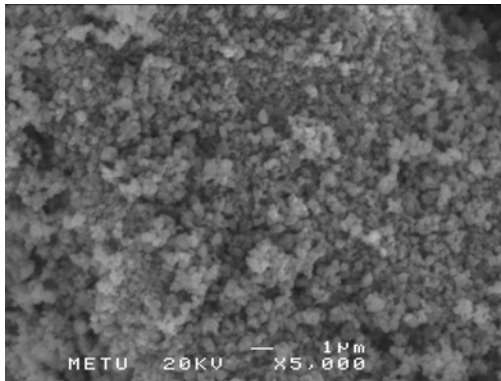

Fig.4.19 SEM micrograph of a MCP sample leached for 3 minutes

In order to see effect of ball milling process for 5 hours on structure of the powders, SEM micrographs of unmilled $Mg + TiO_2 + B_2O_3$ mixture and $Mg + TiO_2 + B_2O_3$ mixture after ball milling process are given Fig.4.20.

<center>(a)   (b)</center>
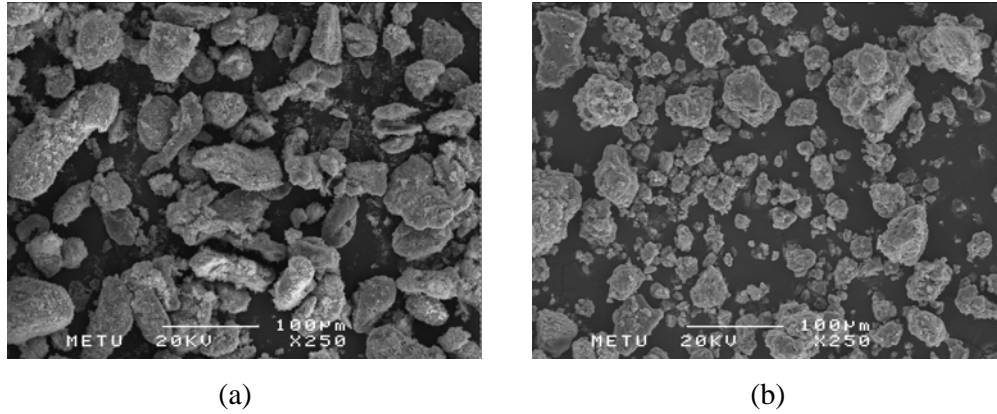
Fig.4.20 SEM micrographs of (a) Mg + TiO$_2$ + B$_2$O$_3$ reactant mixture, (b) Mg + TiO$_2$ + B$_2$O$_3$ reactant mixture after dry ball milling

Fig.4.20(b) indicates that ball milling causes a decrease in particle size of reactants and causes agglomerations. Agglomerates in Fig.4.20(b) are shown in higher magnification in Fig.4.21 where it is seen that the agglomerates are actually composed of smaller reactant particles.

Fig.4.21 Structure of an agglomerate in the Mg + TiO$_2$ + B$_2$O$_3$ reactant mixture after dry ball milling

In order to see the effect of a decrease in particle size on the ignition behavior, sample ball milled for 5 hours was decided to be ignited in the furnace preheated to 800 ^{o}C and then leached in 1 M HCl solution for 15 hours.
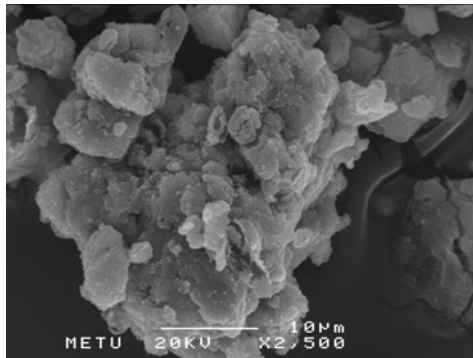
It was observed that ball milling before ignition in the furnace caused a decrease in ignition temperature of the powder mixture containing TiO_2, B_2O_3, and Mg. While without ball milling process ignition temperature was around 690°C, with introduction of ball milling process before ignition, this temperature became approximately 220 ^{o}C. Ignition behaviors of these samples are presented in the Temperature vs. Time plot given in Fig.4.22. The reason of this decrease in ignition temperature may be due to particle size reduction and intimate mixing during ball milling [81-83].
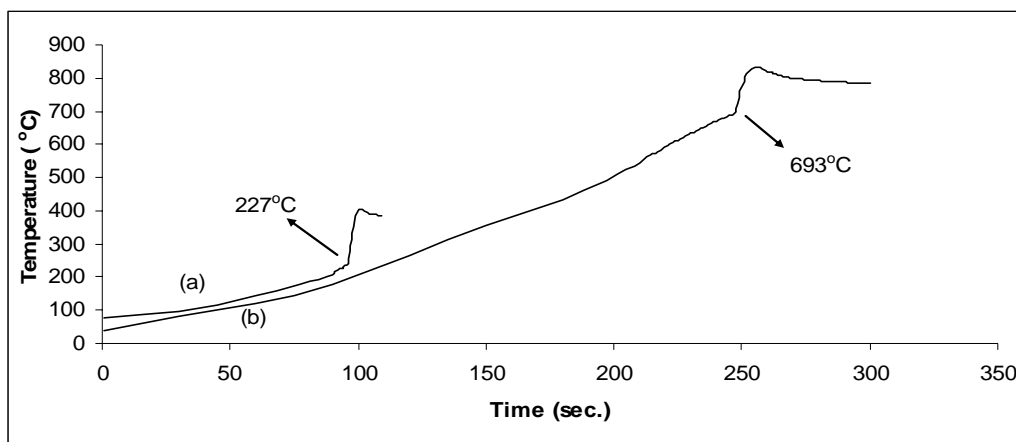
Fig.4.22 Ignition temperatures of (a) Ignited sample after ball milling, (b) Ignited sample without ball milling operation before ignition (plot (a) was shifted 50 ^{o}C up for clarity)

XRD pattern of stoichiometric sample ball milled for 5 hours, ignited in air at 800 ^{o}C and leached in 1 M HCl for 15 hours at room temperature is given in Fig.4.23. As seen from this figure, ignition after ball milling causes a little decrease in $Mg_3B_2O_6$

peaks. The reason of this decrease may be due to mechanical activation of reactant mixture during ball milling because when ball milling is performed before ignition, it causes mechanical activation in which size reduction, mixing and defect formation take place [81-83].
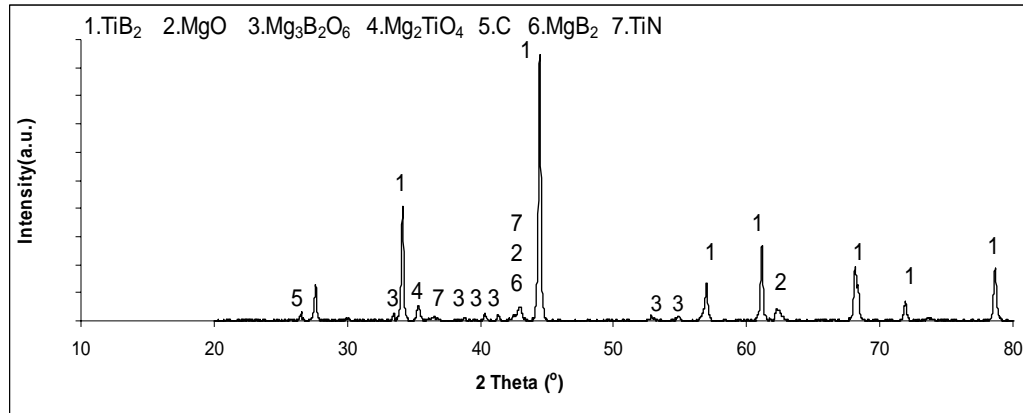
Fig.4.23 XRD pattern of the sample ball milled for 5 h, ignited in air at 800 $^{\circ}$C and leached in 1 M HCl for 15 h at room temperature

SEM micrographs of ignited sample in the furnace preheated to 800 $^{\circ}$C and ignited sample after ball milling for 5 hours with 300 rpm are given in Fig.4.24(a) and Fig.4.24(b), respectively. Since ball milling provides a decrease in particle size, it causes a more vigorous ignition. Porous particles were obtained in this vigorous combustion as it is seen in Fig.4.24(b).
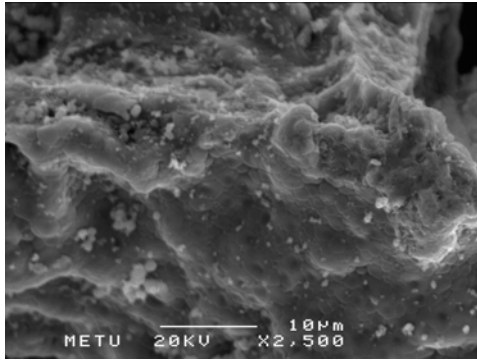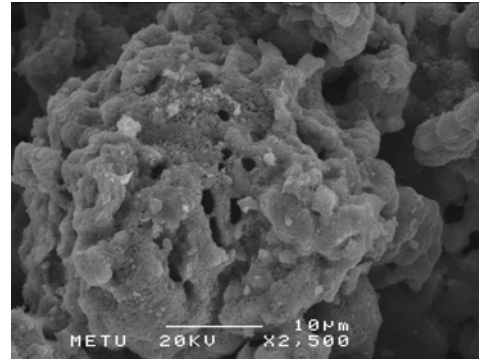
(a)	(b)

Fig.4.24 SEM micrographs of (a) Ignited sample, (b) Ignited sample after ball milling for 5 h

CHAPTER V

CONCLUSIONS

In this study, volume combustion synthesis and mechanochemical processing of B_2O_3 + Mg + TiO_2 and H_3BO_3 + Mg + TiO_2 mixtures were investigated. In volume combustion experiments, it was observed that ignition of H_3BO_3 containing mix took place at 745 ^{o}C while the ignition temperature was 693 ^{o}C with B_2O_3 containing mix. XRD analyses indicated that minor phases, Mg_2TiO_4, $Mg_3B_2O_6$, TiN and MgB_2 were present in the reaction products in addition to the expected TiB_2 and MgO phases. In order to eliminate these side products and MgO, ignited samples, ignited and ball milled samples, and ignited and ethanol ball milled samples were leached in HCl solution with different concentrations at room temperature. In addition, ignited sample was leached at 75°C. It was found that MgO, $Mg_3B_2O_6$ and Mg_2TiO_4 minor phases could be removed after leaching in 3 M HCl solution of ethanol ball milled product. MgB_2 was eliminated after leaching in 5 M HCl solution of ethanol ball milled product. However, TiN could not be removed after HCl leaching. No TiN was observed to form when ignition was conducted under argon atmosphere. In mechanochemical processing experiments, ball milling was performed for 5 and 15 hours under argon atmosphere, and it was observed that after 5 hours of ball milling Reaction (4.2) did not take place. To determine ignition behavior of the 5 hour ball milled reaction mix, it was ignited and it was observed that ignition temperature was decreased to 220 ^{o}C. After 15 hours of ball milling only TiB_2 and MgO was obtained as reaction products and after 3 minutes of leaching in 0.5 M HCl solution MgO

could be removed. As a conclusion, pure titanium diboride was obtained using the following procedures.

1. Ignition of stoichiometric B_2O_3+TiO_2+Mg mix in the furnace preheated to 800 ^{o}C + Ethanol ball milling for 7 hours with 150 rpm + Leaching in 5 M HCl for 15 hours at room temperature. Yield of TiB_2 was 30%.

2. Ignition of stoichiometric B_2O_3+TiO_2+Mg mix in the furnace preheated to 800 ^{o}C + Leaching in 5 M HCl for 15 hours at 75 ^{o}C. Yield of TiB_2 was 45.6%.

3. Ball milling of stoichiometric B_2O_3+TiO_2+Mg mix under argon atmosphere for 15 hours with a speed of 300 rpm + Leaching in 0.5 M HCl for 3 minutes. Yield of TiB_2 was 89.6%.

REFERENCES

[1] W. D. Callister, '*Materials Science and Engineering*', Second Edition, John Wiley & Sons, Inc., New York, 1991.

[2] R. M. Adams, '*Boron, Metallo-Boron Compounds, and Boranes, Edited by Roy M. Adams***,** Interscience Publishers, New York, (1964).

[3] J. Rao et al., Diamond & Related Materials, 13, 2221 (2004).

[4] S. Mollica et al., Surface and Coating Technology, 177-178, 185, (2004).

[5] A. Anal et al., Journal of Materials Processing Technology, 172, 70, (2006).

[6] S. C. Tjong et al., Material Chemistry and Physics, 97, 91, (2006).

[7] P.D. Zavitsanos et al., Ceramic Engineering and Science Proceeding, 4, 624, (1983).

[8] T. Saito et al., Journal of Materials Science, 32, 3933, (1997).

[9] Y. H. Koh et al., Journal of American Ceramic Society, 84, 239, (2001).

[10] A. Kulpa et al., Journal of American Ceramic Society, 79,518, (1996).

[11] S. K. Roy, A. Biswas, Journal of Materials Science Letters, 13, 371, (1994).

[12] L. C. Montgomery et al., '*Process for Producing Titanium Diboride and Boron Nitride Powders*', U. S. Patent No: 5100845, (1992).

[13] V. Sundaram et al., Journal of Materials Research, 12, 2657, (1997).

[14] U. Demircan et al., Materials Research Bulletin, (2006) (in press).

[15] P. Schwarzkopf, '*Refractory Hard Metals: Borides, Carbides, Nitrides, And Silicides; The Basic Constituents Of Cemented Hard Metals And Their Use As High-Temperature Materials by Paul Schwarzkopf and Richard Kieffer in collaboration with Werner Leszynski and Fritz Benesovsky*', New York, Macmillan, (1953).

[16] C. A. Perottoni et al**.,** Journal of Physics. Condensed Matter, 12, 7205, (2000).

[17] M. Schwartz, '*Encyclopedia of Materials, Parts, and Finishes*', CRC Press, New York, (2002).

[18] L. I. Jun et al., Rare Metals, 25, 111, (2006).

[19] W. Xibao et al., Surface and Coatings Technology 137, 209, (2001).

[20] D.D. Radev, Journal of Materials Synthesis and Proccessing, 9, 131, (2001).

[21] G. S. Brady, Henry R. Clauser, J. A. Vaccari, '*Materials Handbook*', McGraw-Hill Com., New York, (2002).

[22] C. Mroz, American Ceramic Society Bulletin, 74, 158, (1995).

[23] R. G. Munro, Journal of Research of the National Institute of Standards and Technology, 105, 709, (2000).

[24] Z. Yuhua et al., Materials Research Bulletin 39, 1615, (2004).

[25] H. H. Hausner, '*Modern Materials Vol.2*', Academic Press, New York, (1960).

[26] S. Mollica et al., Nuclear Instruments and Methods in Physics Research B, 190, 736, (2002).

[27] A. W. Weimer, '*Carbide, Nitride and Boride Materials Synthesis and Processing*', Chapman & Hall, London, (1997).

[28] K. B. Shim et al., Materials Characterization, 31, 39, (1993).

[29] Z. Jiang et al., Journal of European Ceramic Society, 12, 403, (1993).

[30] R. Königshofer et al., International Journal of Refractory Metals and Hard Materials, 23, 350, (2005).

[31] C. Pfohl et al., Surface and Coating Technology, 131, 141, (2000).

[32] R. Kullmer et al., Surface and Coating Technology,174-175, 1229, (2003).

[33] B. Prakash et al., Surface and Coating Technology, 154, 182, (2002).

[34] E. M. Augustine, '*Coated Reinforced Ceramic Cutting Tools*', U. S. Pat. No: 6447896, (1986).

[35] D. Jianxin et al., Journal European Ceramic Society, 25, 1073, (2005).

[36] Trends That Drive Cutting Tool Development, Last Accessed: 01.02.2007, http://www.mmsonline.com/articles/mtg0003.html.

[37] J.A. Sekhar et al., Metallurgical and Materials Transactions B, 29B, 59, (1998)

[38] L. G. Boxall et al., '*Aluminum Cell Cathode Coating Method*', U. S. Patent No: 4466996, 1982.

[39] S. V. Devyatkin et al., Journal of Solid State Chemistry, 154, 107, (2000).

[40] M. Cohen, '*Composite Armor*', U. S. Pat. No: 6203908, (1999).

[41] A. Pettersson et al., International Journal of Impact Engineering, 32, 387, (2005).

[42] Long-Hao Li et al., Journal of European Ceramic Society, 22, 973, (2002).

[43] W. F. Henshaw et al., Ceramic Engineering and Science Proceeding, 4, 634, (1983)

[44] P. D. Zavitsanos et al., Ceramic Engineering and Science Proceeding, 4, 624, (1983)

[45] P. Mossino, Ceramics International, 30, 311, (2004)

[46] L. L. Wang, Journal of Materials Science, 28, 3693, (1993).

[47] B. Aronsson, '*Borides, Silicides, and Phosphides; a Critical Review of Their Preparation, Properties and Crystal Chemistry*', Wiley, London, (1965)**.**

[48] R. L. Sands, '*Powder Metallurgy: Practice and Applications by R. L. Sands and C. R. Shakespeare*', London, (1966).

[49] F. Thümmler, '*An introduction to powder metallurgy / F. Thümmler and R. Oberacker* ', London: Institute of Materials, (1993).

[50] I. E. Campbell, '*High-Temperature Materials and Technology, Edited by Ivor E. Campbell and Edwin M. Sherwood* ', Wiley, New York, (1967).

[51] J. B. Holt et al., Materials Science and Engineering, 71, 321, (1985).

[52] J. J. Kim et al., Ceramic Engineering and Science Proceeding, 6(9,10), 1313, (1985).

[53] R. V. Krishnarao et al., Materials Science and Engineering, A362, 145, (2003).

[54] R. Koc et al., Journal of Materials Science Letters, 19, 667, (2000)

[55] H. M. Greenhouse et al., Journal of American Ceramic Society, 73, 5086, (1951).

[56] J. A. Nelson et al., Journal of Electrochemical Society, 98, 465, (1951).

[57] Y. Taneoka et al., Journal of American Ceramic Society, 72, 1047, (1989).

[58] A. Kurtoğlu, Master Thesis, METU, Ankara, August 2004.

[59] M. Elmadağlı, Master Thesis, METU, Ankara, July 2000.

[60] L. Y. Markovskii et al., Power Metallurgy and Metal Ceramics, 8, 350, (1969).

[61] K. V. Logan, '*Process for Making Highly Reactive Sub-micron Amorphous Titanium Diboride Powder and Products Made Therefrom*', U. S. Patent No: 5160716, (1989).

[62] K.V. Logan, '*Material Made From Highly Reactive Sub-Micron Amorphous Titanium Diboride Powder and Products Made Therefrom*', U. S. Patent No: 5275781, (1994).

[63] V. Sundaram et al., British Ceramic Society Transactions, 56, 111, (1995).

[64] W. Weimin et al., Journal of Materials Processing Technology, 128, 162, (2002).

[65] N. J. Welham, Journal of American Ceramic Society, 83, 1290, (2000).

[66] R. Ricceri et al., Materials Science and Engineering, A 379, 341, (2004).

[67] G. Kaptay et al., Plasma and Ions, 2, 45, (1999).

[68] M. Makyta et al., Journal of Applied Electrochemistry, 26, 319, (1996).

[69] M. Makyta et al., Light Metals (U. S.), 1137, (1993).

[70] D. Schlain et al., Journal of Electrochemical Society, 16, 1227, (1969).

[71] I. E. Campbell et al., Journal of Electrochemical Society, 96, 318, (1949).

[72] J. Brynestad et al., High Temperature Science, 19, 41, (1985).

[73] C. Suryanarayana, '*Mechanical Alloying and Milling*', Marcel Dekker, New York, (2004).

[74] N. J. Welham, Mineral Engineering, 12, 1213, (1999).

[75] Y. Hwang et al., Materials Letters, 54, 1, (2002).

[76] Retsch PM 100, '*Operating Intstructions Ball Mills*', Retsch GmbH Com., (2003).

[77] G.V. Arsdale, '*Hydrometallurgy of Base Metals*', The Maple Press Com., Inc., New York, (1953).

[78] F. Habashi, '*Principles of Extractive Metallurgy Volume 2 Hydrometallurgy*' Gordon and Breach Science Publishers Ltd., New York, London, Paris, (1970).

[79] B. D. Cullity, S. R. Stock, '*Elements of X-Ray Diffraction*', Prentice Hall, New Jersey, (2001).

[80] S. V. Gurov et al., Powder Metallurgy and Metal Ceramics, 24, 607, (1985).

[81] L. Takacs, Progress in Materials Science, 47, 355, (2002).

[82] F. Maglia et al., Journal of Materials Research, 16, 1074, (2001).

[83] U. Anselmi-Tamburini, Journal of Material Synthesis and Processing, 8, 377, (2000).